Supporting Information

Encapsulation of a Ruthenium-Platinum Photosensitizer into Nanofibrous Membranes for Antibacterial Photodynamic Therapy

Santanu Patra,[a#] Zisis Papadopoulos,[b#] Juan Sanz-Villafruela,[b] Johannes Karges,[b*] Anzhela Galstyan [a, c *]

a. Faculty of Chemistry, University of Duisburg-Essen, Universitätsstraße 5, Essen, 45141 Germany
b. Department of Biophysics, Faculty of Medicine, Ruhr University Bochum, Universitätsstrasse 150, 44801 Bochum.
c. Center for Protein Diagnostics (PRODI), Ruhr University Bochum, Gesundheitscampus 4, 44801 Bochum, Germany
d. Center for Nanointegration Duisburg-Essen (CENIDE), Center of Medical Biotechnology (ZMB) and Center for Water and Environment Research (ZWU), Universitätsstraße 5, Essen, 45141 Germany, Email: anzhela.galstyan@uni-due.de
# These authors contributed equally to this work.

Table of Contents

EXPERIMENTAL SECTION

1. Materials and Methods

Ruthenium(III)-chloride hydrate ($RuCl_3 \cdot xH_2O$) and potassium tetrachloroplatinate(II) ($K_2[PtCl_4]$) were purchased from Johnson Matthey and used as received. The reagents tryptamine, 5-bromo-2-pyridinecarboxaldehyde, tetrabutylammonium fluoride (TBAF) and activated manganese dioxide (MnO_2), were purchased from Sigma-Aldrich; sodium hydride (NaH), methyl iodide, (triisopropylsilyl)acetylene, tetrakis(triphenylphosphine)palladium(0) ($Pd(PPh_3)_4$), triethylamine (NEt_3), 2,2'-bipyrydine (bipy), 2, 2′:6′, 2′-terpyridine (terpy) and copper(I) iodide (CuI) were purchased from TCI Chemicals. All of them were used without further purification. Deuterated dimethyl sulfoxide (DMSO-d_6) and deuterated chloroform ($CDCl_3$) were obtained from Eurisotop. All solvents used were analytical or high-performance liquid chromatography (HPLC) grade. In some cases they were dried prior to use. UV-vis absorption spectra were measured on a Shimadzu UV-1800 spectrometer in a 1 cm quartz cuvette. Integrating sphere measurements were carried out on a Shimadzu UV-2600i UV-vis spectrometer. Fluorescence and phosphorescence spectra were measured on a Horiba Fluoromax+ spectrometer with a R928P photon counting PMT Detector or DSS IR FLIGA 1.7 with the possibility for liquid nitrogen cooling. The membrane morphology was examined by scanning electron microscopy (SEM) with an Apreo S LoVac instrument (Thermo Fisher Scientific, Waltham, MA, USA).

2. Synthesis and Characterization

2.1 Synthetic procedures

All synthetic procedures employed for the synthesis of RuPt were originally reported in our previous publication.[1]

1-(5-bromopyridin-2-yl)-β-carboline

1-(5-bromopyridin-2-yl)-β-carboline was prepared following the procedure reported in our previous work.[1] A mixture of tryptamine (0.40 g, 2.50 mmol), 5-bromo-2- pyridine carboxaldehyde (0.47 g, 2.50 mmol) and 80 mL of dry anisole was stirred at 160 °C for 3 h. After 3 h, the mixture was allowed to reach room temperature and activated MnO_2 (25 equiv.) was added. The mixture was stirred at 160 °C for 21 h. Thereafter, the mixture was filtered over Celite while hot and solvent was removed under vacuum. The resulting grey solid was washed with hexane (2 × 10 mL) and dried under vacuum. Yield: 0.73 g (90%). ^{1}H-NMR (300 MHz, DMSO-d_6): δ = 11.83 (s, 1H), 8.92 (dd, *J* = 2.4, 0.6 Hz, 1H), 8.55 (dd, *J* = 8.6, 0.6 Hz, 1H), 8.49 (d, *J* = 5.1 Hz, 1H), 8.39 – 8.20 (m, 3H), 7.84 (d, *J* = 8.1 Hz, 1H), 7.58 (t, *J* = 7.7 Hz, 1H), 7.28 (t, *J* = 7.5 Hz, 1H) ppm. ^{13}C-NMR (75 MHz, DMSO-d_6): δ =155.8, 149.2, 141.1, 139.9, 137.9, 137.1, 133.4, 130.1, 128.5, 122.7, 121.7, 120.3, 119.7, 119.7, 116.1, 112.9 ppm. ESI-HRMS (pos. detection mode): calcd for $C_{16}H_{11}BrN_3$ $[M+H]^+$ m/z 324.0136; found: 324.0147. Elemental analysis calcd for $C_{16}H_{10}BrN_3 \cdot (H_2O)_{0.3}$ (%): C 58.31, H 3.24, N 12.75; found: C 58.32, H 3.19, N 12.28.

1-(5-bromopyridin-2-yl)-9-methyl-β-carboline

1-(5-bromopyridin-2-yl)-9-methyl-β-carboline was prepared following the procedure reported in our previous work.[1] A suspension of 1-(5-bromopyridin-2-yl)-β-carboline (1.000 g, 3.08 mmol) in anhydrous *N*,*N*-dimethylformamide (40 mL) was stirred at 0 °C for five minutes. Then, 60% sodium hydride (185 mg, 4.63 mmol) was added. The mixture was allowed to reach room temperature and stirred for 1 h. After 1 h, the mixture was cooled to -10 °C and methyl iodide (250 µL, 4.0 mmol) was added dropwise. Thereafter, the mixture was allowed to reach room temperature and stirred overnight. Then, the solution was cooled to 0 °C and 30 mL of distilled water were added dropwise to neutralize the excess of sodium hydride. The resulting grey solid was filtered and washed with hexane (2 × 10 mL) and dried under vacuum. Yield: 1.05 g (96%). ^{1}H-NMR (300 MHz, DMSO-d_6): δ = 8.87 (d, *J* = 2.4 Hz, 1H), 8.46 (d, *J* = 5.1 Hz, 1H), 8.33 (d, *J* = 7.8 Hz, 1H), 8.33 – 8.19 (m, 2H), 7.98 (d, *J* = 8.4 Hz, 1H), 7.76 – 7.58 (m, 2H), 7.32 (t, *J* = 8.0 Hz, 1H), 3.56 (s, 3H). ^{13}C-NMR (300 MHz, DMSO-d_6): δ = 156.5, 148.8, 142.5, 141.2, 139.6, 137.9, 134.7, 130.1, 128.8, 126.7, 121.7, 120.3, 119.9, 115.0, 110.5, 33.6 ppm. ESI-HRMS (pos. detection mode): calcd for $C_{17}H_{13}BrN_3$ $[M+H]^+$ m/z 338.0293; found: 338.0292. Elemental analysis calcd for $C_{17}H_{12}BrN_3$ (%): C 60.37, H 3.58, N 12.42; found: C 60.17, H 3.64, N 12.20.

9-methyl-1-(5-((triisopropylsilyl)ethynyl)pyridin-2-yl)-β-carboline

9-methyl-1-(5-((triisopropylsilyl)ethynyl)pyridin-2-yl)-β-carboline was prepared following the procedure reported in our previous work.[1] 1-(5-bromopyridin-2-yl)-9-methyl-β-carboline (0.54 g, 1.60 mmol), tetrakis(triphenylphosphine)palladium(0) (10 mol %) and copper(I) iodide (10 mol %) were added in a 100 mL Schlenk flask under nitrogen flow. Then, 35 mL of dry and

deoxygenated *N*,*N*-dimethylformamide, triethylamine (2.23 mL, 16 mmol) and (triisopropylsilyl)acetylene (0.54 mL, 2.4 mmol) were added. The mixture was heated overnight at 65 °C. Afterwards, solvent was removed, and the solid was extracted with dichloromethane (3 × 20 mL). The organic layers were combined, dried over anhydrous magnesium sulfate and filtered. Finally, the solvent was removed, and the product was purified by column chromatography on silica using dichloromethane:methanol (98:2) as mobile phase yielding a white solid. Yield: 0.45 g (63%). ^{1}H-NMR (500 MHz, $CDCl_3$): δ = 8.84 (d, *J* = 1.1 Hz, 1H), 8.54 (d, *J* = 5.0 Hz, 1H), 8.17 (dd, *J* = 7.8, 1.1 Hz, 1H), 8.03 (d, *J* = 5.1 Hz, 1H), 8.00 (dd, *J* = 8.1, 0.9 Hz, 1H), 7.96 (dd, *J* = 8.1, 2.0 Hz, 1H), 7.62 (t, *J* = 7.7 Hz, 1H), 7.46 (d, *J* = 8.3 Hz, 1H), 7.31 (t, *J* = 7.4 Hz, 1H), 3.64 (s, 3H), 1.19 – 1.17 (m, 21H) ppm. ^{13}C-NMR (126 MHz, $CDCl_3$): δ = 157.15, 151.24, 143.19, 141.73, 139.65, 138.32, 135.51, 131.20, 128.67, 124.33, 121.44, 121.11, 119.91, 119.74, 114.72, 109.96, 103.56, 95.78, 33.91, 18.70, 11.31 ppm. ESI-HRMS (pos. detection mode): calcd for $C_{28}H_{34}N_3Si$ $[M+H]^+$ m/z 440.2522; found: 440.2516. Elemental analysis calcd for $C_{28}H_{33}N_3Si$ (%): C 76.49, H 7.57, N 9.56; found: C 76.25, H 7.64, N 9.64.

[Ru(2,2'-bipyridine)$_2$Cl$_2$]

[Ru(2,2'-bipyridine)$_2$Cl$_2$] was synthesized using a synthetic protocol described in literature.[2] Ruthenium(III)-chloride hydrate (1.00 g, 3.82 mmol, assuming xH_2O = 3), 2,2'-bipyridine (1.21 g, 7.72 mmol), and lithium chloride (1.13 g, 26.74 mmol) were heated at reflux in *N*,*N*-dimethylformamide (7 mL) for 8 h. The reaction was stirred magnetically throughout this period. Then, the mixture was cooled to room temperature and 32 mL of acetone were added. The solution was cooled at 0 °C overnight yielding a dark green-black micro-crystalline product. The solid was collected by filtration and washed with water (3 × 5 mL) and diethyl ether (3 × 10 mL). Finally, the solid was dried under vacuum. Yield: 0.98 g (53%). ^{1}H-NMR (500 MHz, DMSO-d_6): δ = 9.96 (d, *J* = 5.4 Hz, 2H), 8.63 (d, *J* = 8.0 Hz, 2H), 8.47 (d, *J* = 8.2 Hz, 2H), 8.06 (t, *J* = 7.4 Hz, 2H), 7.76 (t, *J* = 6.3 Hz, 2H), 7.66 (t, *J* = 7.6 Hz, 2H), 7.50 (d, *J* = 5.7 Hz, 2H), 7.10 (t, *J* = 6.6 Hz, 2H) ppm. ^{13}C-NMR (126 MHz, DMSO-d_6): δ = 160.22, 158.17, 153.16, 152.02, 134.59, 133.38, 125.36, 125.24, 122.82, 122.51 ppm. Elemental analysis calcd for $C_{20}H_{16}Cl_2N_4Ru$ (%): C 49.60, H 3.33, N 11.57; found: C 49.48, H 3.36, N 11.32.

[Ru(2,2'-bipyridine)$_2$(9-methyl-1-(5-((triisopropylsilyl)ethynyl)pyridin-2-yl)-β-carboline)][PF$_6$]$_2$

This complex was prepared following the procedure reported in our previous work.[1] In a 100 mL round-bottom pressure flask, 9-methyl-1-(5-((triisopropylsilyl)ethynyl)pyridin-2-yl)-β-carboline (99.8 mg, 0.227 mmol) and [Ru(2,2'-bipyridine)$_2$Cl$_2$] (100 mg, 0.206 mmol) were suspended in 25 mL of ethanol:water (1:1). The mixture was deoxygenated bubbling nitrogen for 20 minutes. Then, the mixture was heated at 120 °C with continuous magnetic stirring for 24 h. The reaction mixture was cooled to room temperature and ethanol was removed under vacuum. The solution was filtered over Celite, and an excess of ammonium hexafluorophosphate was added to precipitate the product as an orange solid. The solid was collected by filtration and washed with water (2 × 3 mL). Thereafter, the solid was dissolved in the minimum amount of acetonitrile and precipitated with diethyl ether (20 mL). The solid was filtered, washed with diethyl ether (3 × 10 mL) and dried under vacuum for 6 hours yielding an orange solid. The compound was used without further purification. Yield: 195 mg (75%). ^{1}H-

NMR (500 MHz, DMSO-d_6): δ = 8.91 (d, *J* = 4.4 Hz, 1H), 8.88 (d, *J* = 4.5 Hz, 1H), 8.83 (d, *J* = 8.4 Hz, 1H), 8.78 (d, *J* = 8.2 Hz, 1H), 8.35 (d, *J* = 7.9 Hz, 1H), 8.33 – 8.27 (m, 2H), 8.25 – 8.15 (m, 5H), 8.10 (td, *J* = 7.9, 1.4 Hz, 1H), 7.89 – 7.76 (m, 5H), 7.60 – 7.53 (m, 3H), 7.52 – 7.44 (m, 4H), 3.91 (s, 3H), 1.04 – 0.99 (m, 21H) ppm.

[Ru(2,2'-bipyridine)$_2$(1-(5-ethynylpyridin-2-yl)-9-methyl-β-carboline][PF$_6$]$_2$

This complex was prepared following the procedure reported in our previous work.[1] [Ru(2,2'-bipyridine)2(9-methyl-1-(5-((triisopropylsilyl)ethynyl)pyridin-2-yl)-β-carboline)][PF_6]$_2$ (150 mg, 0.131 mmol) was added under a nitrogen flow into a 100 mL Schlenk flask and dissolved in 10 mL of deoxygenated acetonitrile. Subsequently, 5 mL of a THF solution containing tetra-n-butylammonium fluoride (5 equiv.) and acetic acid (0.2 mL) were added. The mixture was stirred overnight at room temperature. Then, an excess of ammonium hexafluorophosphate was added and solvent was removed. Afterwards, 10 mL of water were added and the compound was extracted with dichloromethane (3 × 20 mL). The organic layers were collected, dried over anhydrous magnesium sulfate and filtered. Solvent was removed and the solid was purified by column chromatography on neutral alumina using dichloromethane:methanol (97:3) as mobile phase yielding an orange solid. Yield: 79 mg (61%). ^{1}H-NMR (500 MHz, DMSO-d_6): δ = 8.91 (d, *J* = 8.2 Hz, 2H), 8.86 (d, *J* = 8.2 Hz, 1H), 8.81 (d, *J* = 8.1 Hz, 1H), 8.36 (d, *J* = 8.2 Hz, 2H), 8.31 (d, J = 5.7 Hz, 1H), 8.24 (d, J = 8.6 Hz, 1H), 8.22 – 8.22 – 8.16 (m, 3H), 8.14 (d, *J* = 5.6 Hz, 1H), 8.11 (t, *J* = 7.9 Hz, 1H), 7.87 (d, *J* = 8.4 Hz, 1H), 7.85 – 7.77 (m, 3H), 7.75 (s, 1H), 7.72 (d, J = 5.6 Hz, 1H), 7.60 – 7.43 (m, 6H), 4.74 (s, 1H), 3.93 (s, 3H) ppm. ^{13}C-NMR (126 MHz, DMSO-d_6): δ = 156.8, 156.7, 156.6, 156.4, 156.3, 152.7, 151.9, 151.6, 151.1, 145.6, 140.6, 140.2, 139.4, 138.3, 137.99, 137.96, 137.8, 133.3, 130.9, 127.9, 127.9, 127.8, 127.6, 124.61, 124.56, 124.4, 124.2, 122.4, 122.1, 120.6, 120.3, 118.7, 112.1, 87.8, 78.7, 36.8 ppm. ESI-HRMS (pos. detection mode): calcd for $C_{39}H_{29}N_7Ru$ [M-2PF6]$^{2+}$ m/z 348.5764, found 348.5764; calcd for $C_{39}H_{29}F_6N_7PRu$ [M-PF_6]+ m/z 842.1169, found 842.1186. Elemental analysis calcd for $C_{39}H_{29}F_{12}N_7P_2Ru$ (%): C 47.47, H 2.96, N 9.94; found: C 47.81, H 3.12, N 9.81.

[Ru(2,2'-bipyridine)$_2$(1-(5-ethynylpyridin-2-yl)-9-methyl-β-carboline)Pt(2,2':6',2'-terpyridine)][PF$_6$]$_3$ (RuPt)

This complex was prepared following the procedure reported in our previous work.[1] [Ru(2,2'-bipyridine)$_2$(1-(5-ethynylpyridin-2-yl)-9-methyl-β-carboline][PF_6]$_2$ (100 mg, 0.102 mmol), [Pt(2,2':6',2'-terpyridine)Cl][Cl] (53.4 mg,1.07 mmol), CuI (2 mg, 0.011 mmol) and NEt_3 (2 mL) were added under a nitrogen flow into a 100 mL Schlenk flask containing 10 mL of dry deoxygenated *N*,*N*-dimethylformamide. The mixture was stirred at room temperature for 72 h. Then, an excess of potassium hexafluorophosphate was added and the solvent was removed under vacuum. The solid was washed with water (3 × 5 mL). Solvent was removed and the solid was purified by column chromatography on silica using acetonitrile:water:saturated potassium hexafluorophosphate aqueous solution (95:6:1) as mobile phase. Pure fractions were collected and the solvent was removed under vacuum. The solid was dissolved in the minimum amount of acetonitrile and 20 mL of water were added to obtain a red precipitate. The solid was collected and washed several times with water (3 × 10 mL), ethanol (3 × 2 mL) and diethyl ether (3 × 2 mL). Finally, the red solid was dried under vacuum for 6 hours. Yield: 90 mg (57%). ^{1}H-NMR (500 MHz, DMSO-d_6): δ = 8.99 – 8.95 (m, 2H), 8.91 (d, *J* = 3.8 Hz, 1H), 8.90 (d, *J* =

3.8 Hz, 1H), 8.85 (d, *J* = 8.6 Hz, 1H), 8.82 (d, *J* = 8.3 Hz, 1H), 8.75 – 8.69 (m, 4H), 8.67 – 8.62 (m, 1H), 8.56 (td, *J* = 7.9, 1.5 Hz, 2H), 8.39 – 8.34 (m, 2H), 8.31 – 8.26 (m, 2H), 8.24 – 8.17 (m, 3H), 8.14 (t, *J* = 7.9 Hz, 1H), 8.09 (d, *J* = 5.0 Hz, 1H), 7.93 – 7.85 (m, 5H), 7.82 (t, *J* = 7.4 Hz, 1H), 7.76 (d, *J* = 5.9 Hz, 1H), 7.68 (d, *J* = 2.0 Hz, 1H), 7.62 (t, *J* = 6.6 Hz, 1H), 7.60 – 7.56 (m, 1H), 7.54 – 7.43 (m, 4H), 3.94 (s, 3H) ppm. ^{13}C-NMR (126 MHz, DMSO-d_6): δ = 158.7, 156.9, 156.72, 156.65, 156.5, 154.0, 153.9, 153.7, 152.7, 151.8, 151.7, 151.5, 151.2, 145.7, 142.6, 142.5, 140.9, 140.5, 138.9, 137.9, 137.8, 133.2, 130.8, 129.6, 127.93, 127.90, 127.8, 127.6, 126.1, 125.1, 124.6, 124.5, 124.4, 124.32, 124.29, 122.3, 122.1, 120.7, 118.1, 112.1, 109.9, 98.8, 36.8 ppm. ^{195}Pt-NMR (107 MHz, DMSO-d_6): δ = -3134.10 ppm. ESI-HRMS (pos. detection mode): calcd for $C_{54}H_{39}N_{10}PtRu$ $[M\text{-}3PF_6]^{3+}$ m/z 374.7350, found 374.7366; calcd for $C_{54}H_{39}F_6N_{10}PPtRu$ $[M\text{-}2PF_6]^{2+}$ m/z 634.5844, found 634.5857; calcd for $C_{54}H_{39}F_{12}N_{10}P_2PtRu$ $[M\text{-}PF_6]^{+}$ m/z 1414.1334, found 1414.1340. Elemental analysis calcd for $C_{54}H_{39}F_{18}N_{10}P_3PtRu$ (%): C 41.60, H 2.52, N 8.98; found: C 41.85, H 2.80, N 8.58.

2.2 NMR Data

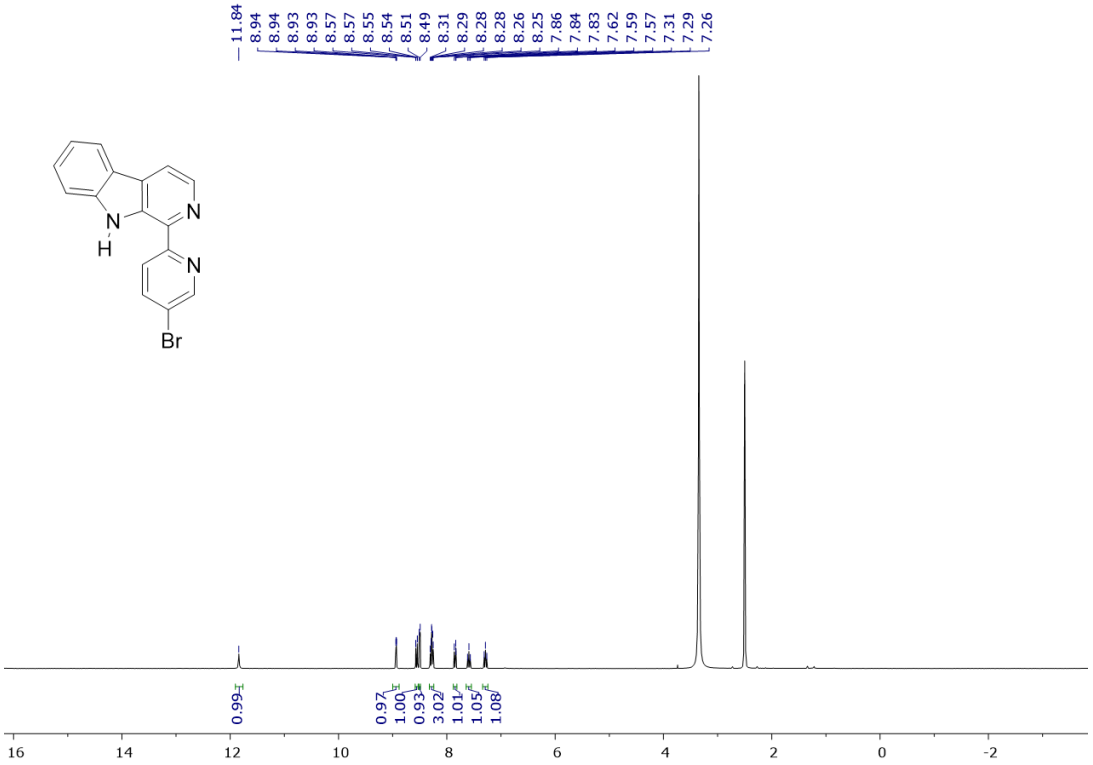

Fig. S1. ^{1}H-NMR (300 MHz, DMSO-d_6) spectrum of 1-(5-bromopyridin-2-yl)-β-carboline.

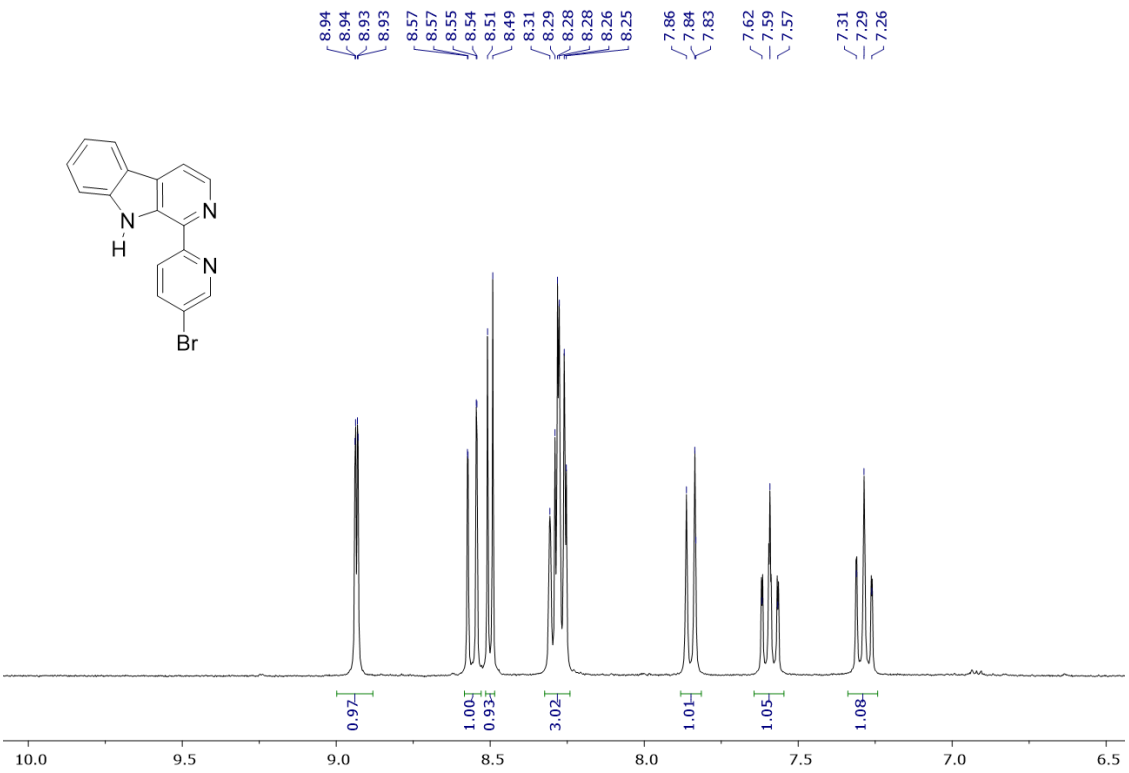

Fig. S2. ^{1}H-NMR (300 MHz, DMSO-d_6) spectrum of 1-(5-bromopyridin-2-yl)-β-carboline in the aromatic region.

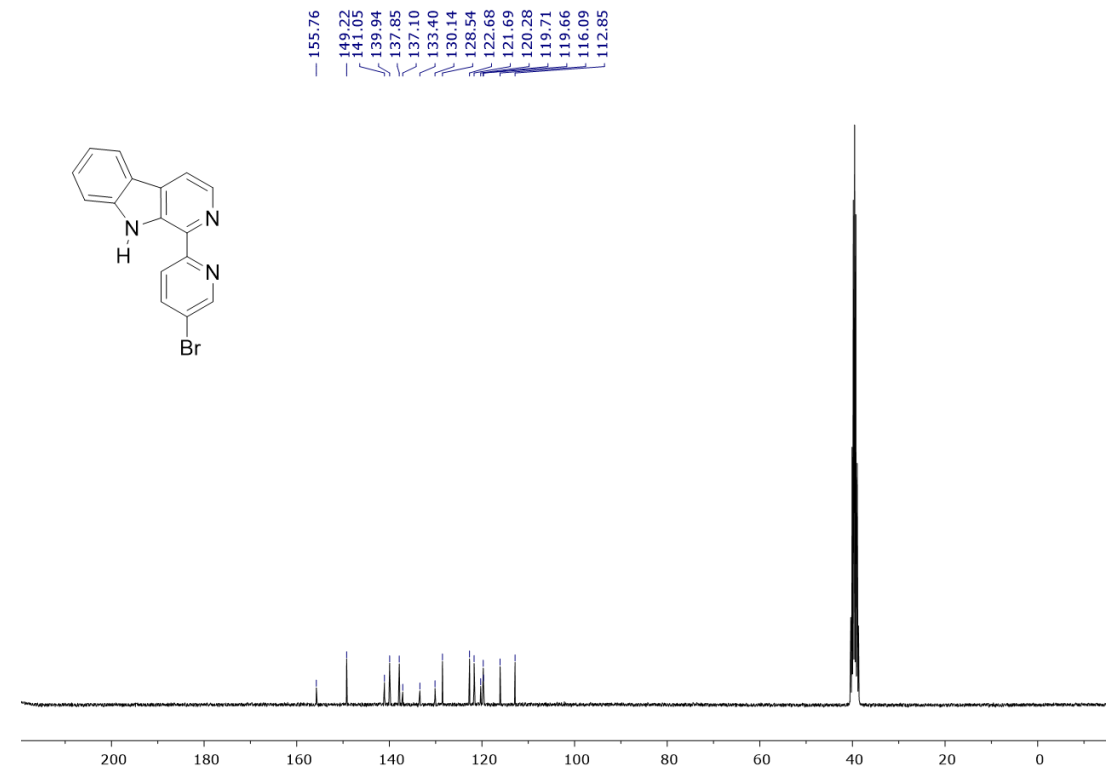

Fig. S3. ^{13}C-NMR (75 MHz, DMSO-d_6) spectrum of 1-(5-bromopyridin-2-yl)-β-carboline.

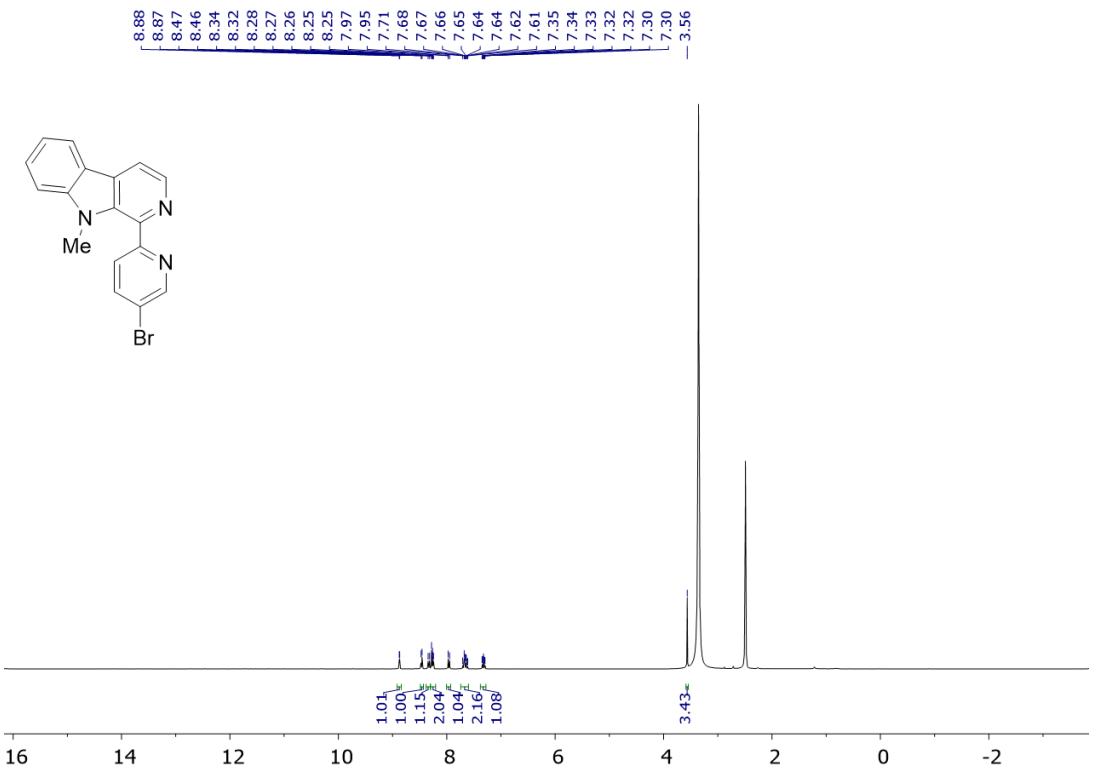

Fig. S4. ^{1}H-NMR (300 MHz, DMSO-d_6) spectrum of 1-(5-bromopyridin-2-yl)-9-methyl-β-carboline.

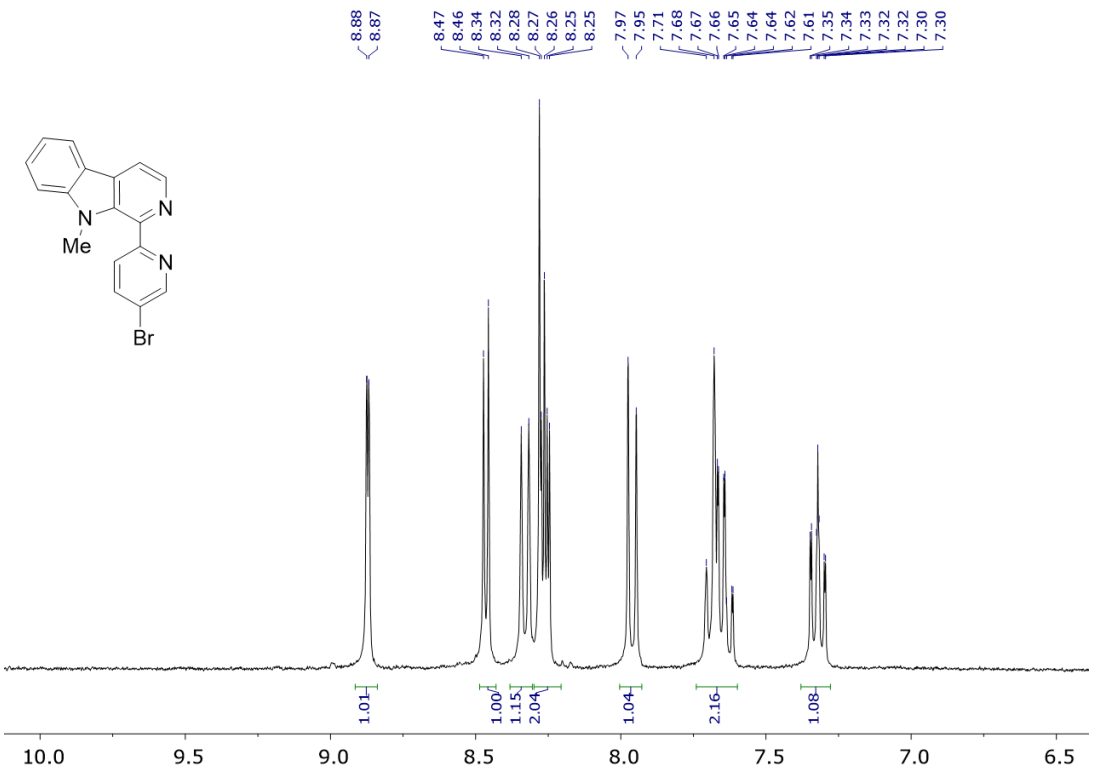

Fig. S5. ^{1}H-NMR (300 MHz, DMSO-d_6) spectrum of 1-(5-bromopyridin-2-yl)-9-methyl-β-carboline in the aromatic region.

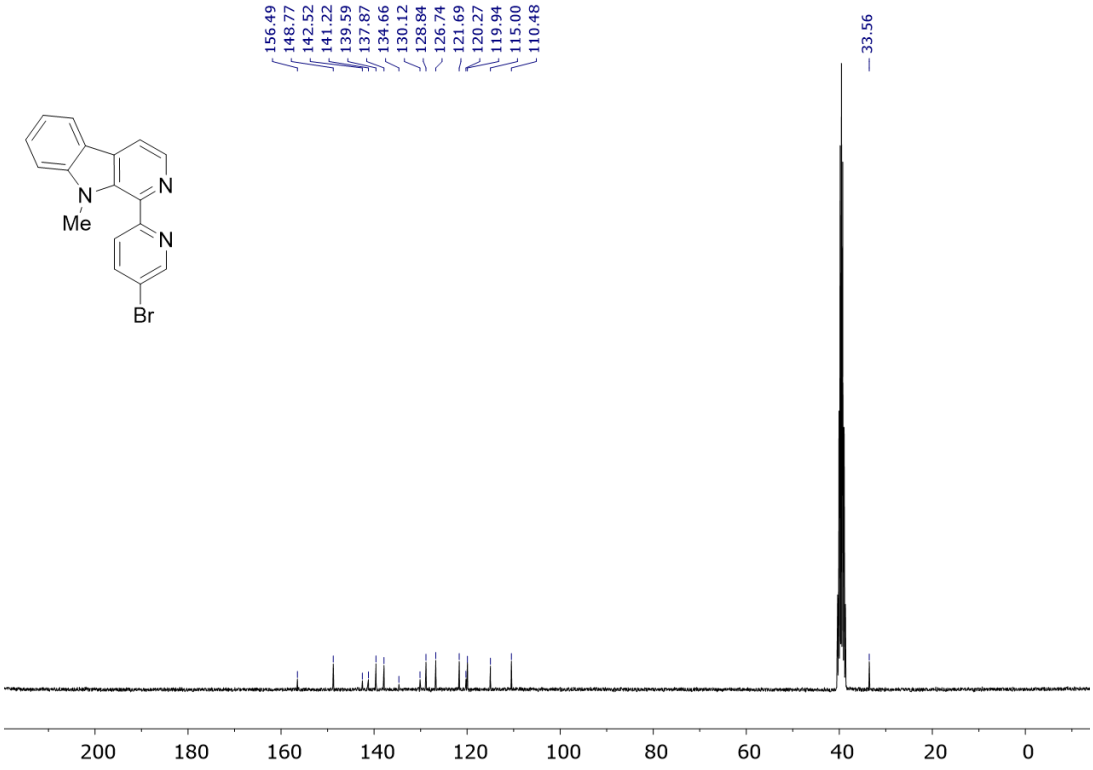

Fig. S6. ^{13}C-NMR (75 MHz, DMSO-d_6) spectrum of 1-(5-bromopyridin-2-yl)-9-methyl-β-carboline.

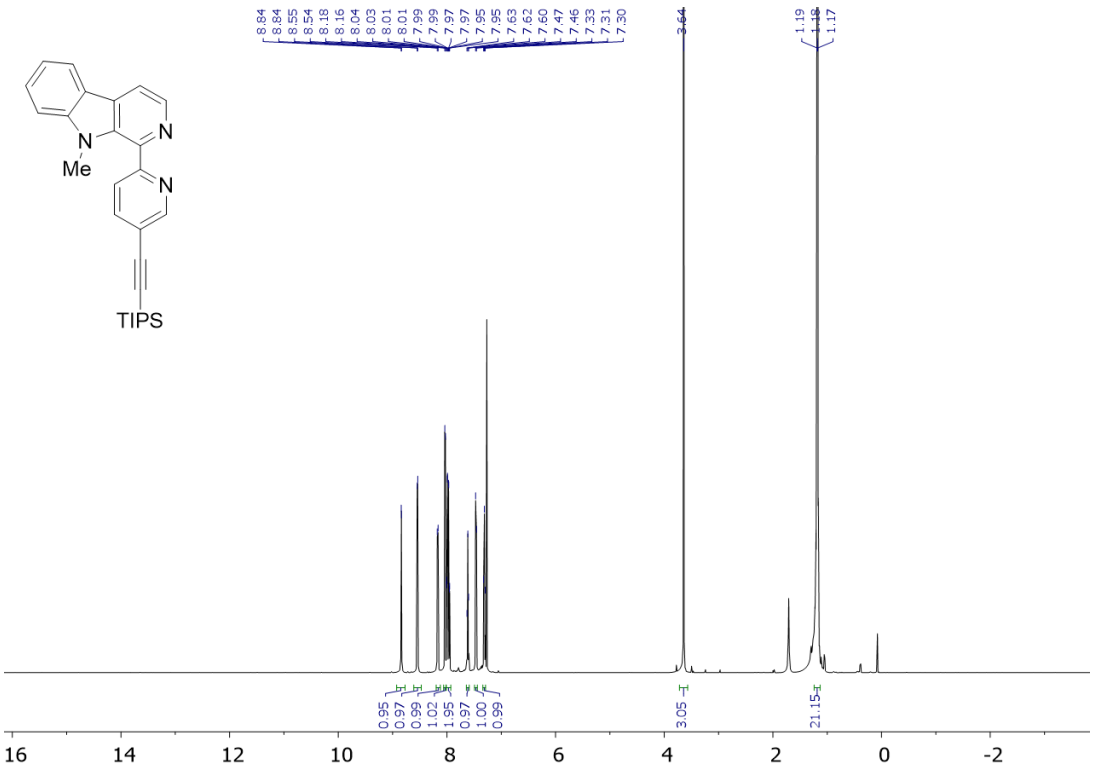

Fig. S7. ^{1}H-NMR (500 MHz, $CDCl_3$) spectrum of 9-methyl-1-(5-((triisopropylsilyl)ethynyl)pyridin-2-yl)-β-carboline.

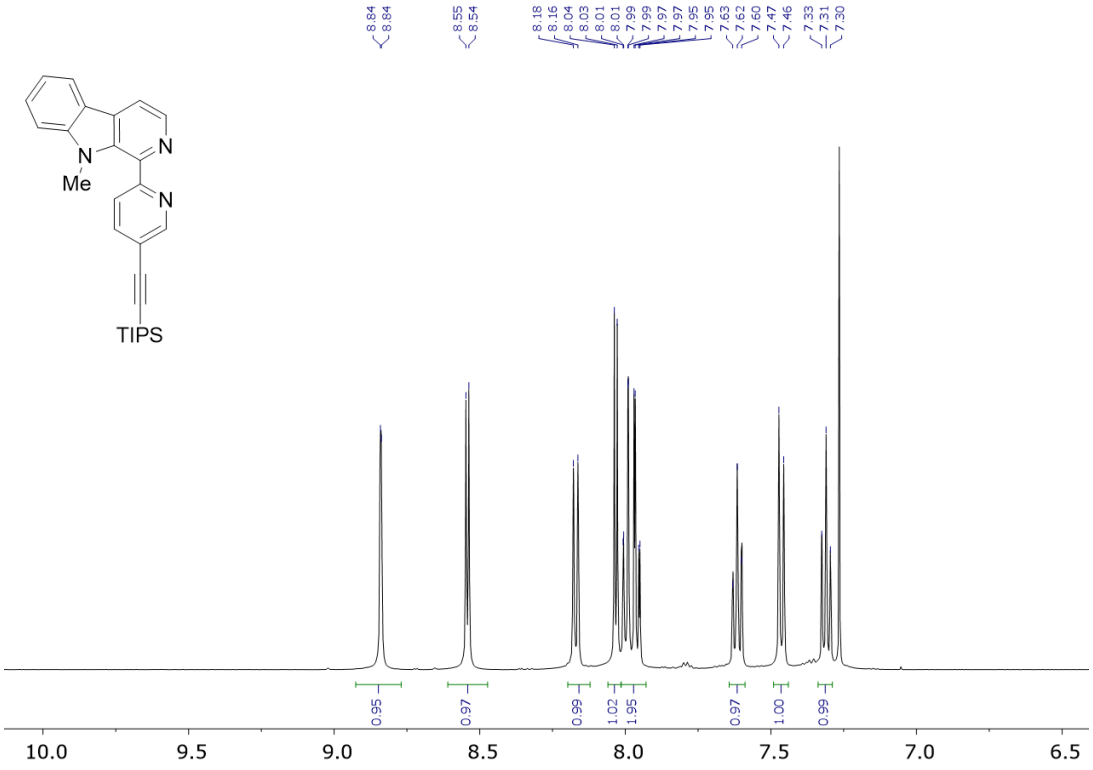

Fig. S8. ^{1}H-NMR (500 MHz, $CDCl_3$) spectrum of 9-methyl-1-(5-((triisopropylsilyl)ethynyl)pyridin-2-yl)-β-carboline in the aromatic region.

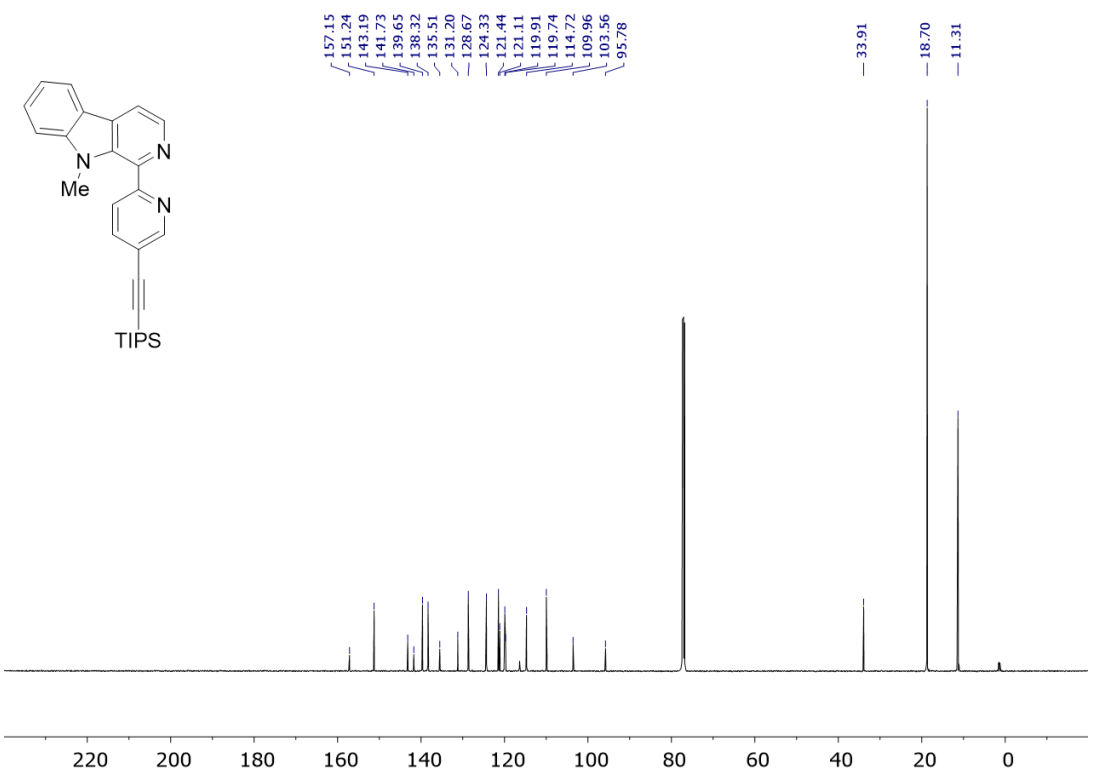

Fig. S9. ^{13}C-NMR (126 MHz, $CDCl_3$) spectrum of 9-methyl-1-(5-((triisopropylsilyl)ethynyl)pyridin-2-yl)-β-carboline.

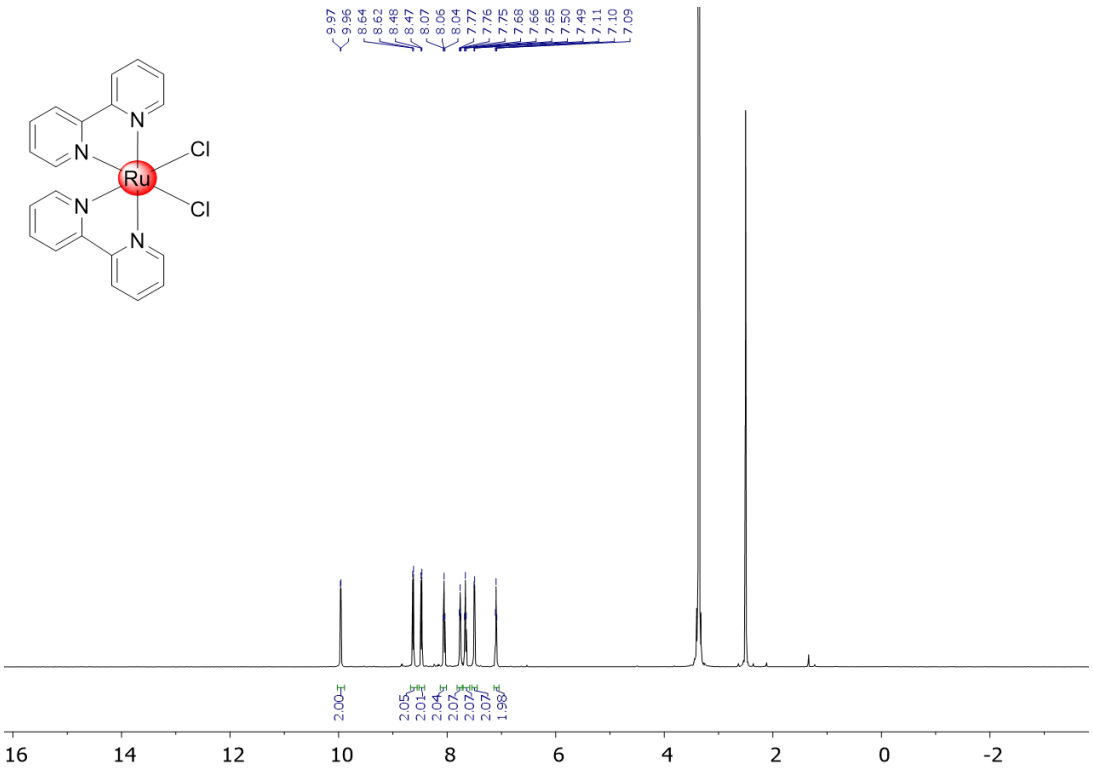

Fig. S10. ^{1}H-NMR (500 MHz, DMSO-d_6) spectrum of [Ru(2,2'-bipyridine)$_2$Cl$_2$].

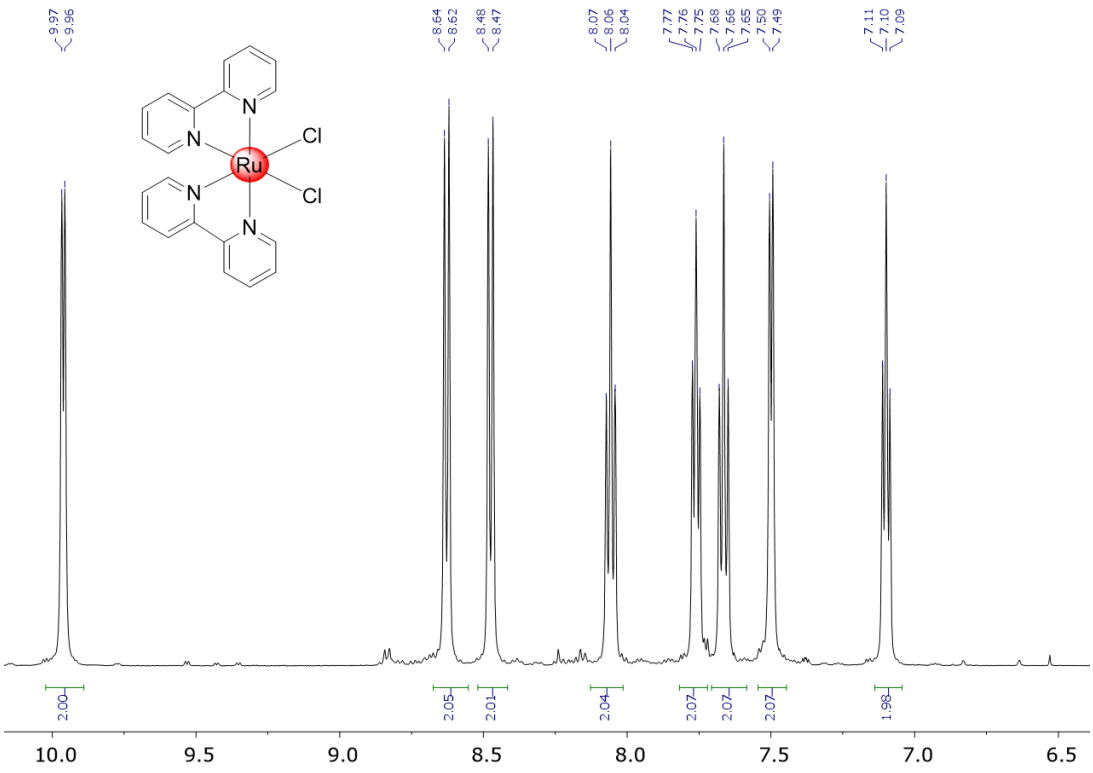

Fig. S11. ^{1}H-NMR (500 MHz, DMSO-d_6) spectrum of [Ru(2,2'-bipyridine)$_2$Cl$_2$] in the aromatic region.

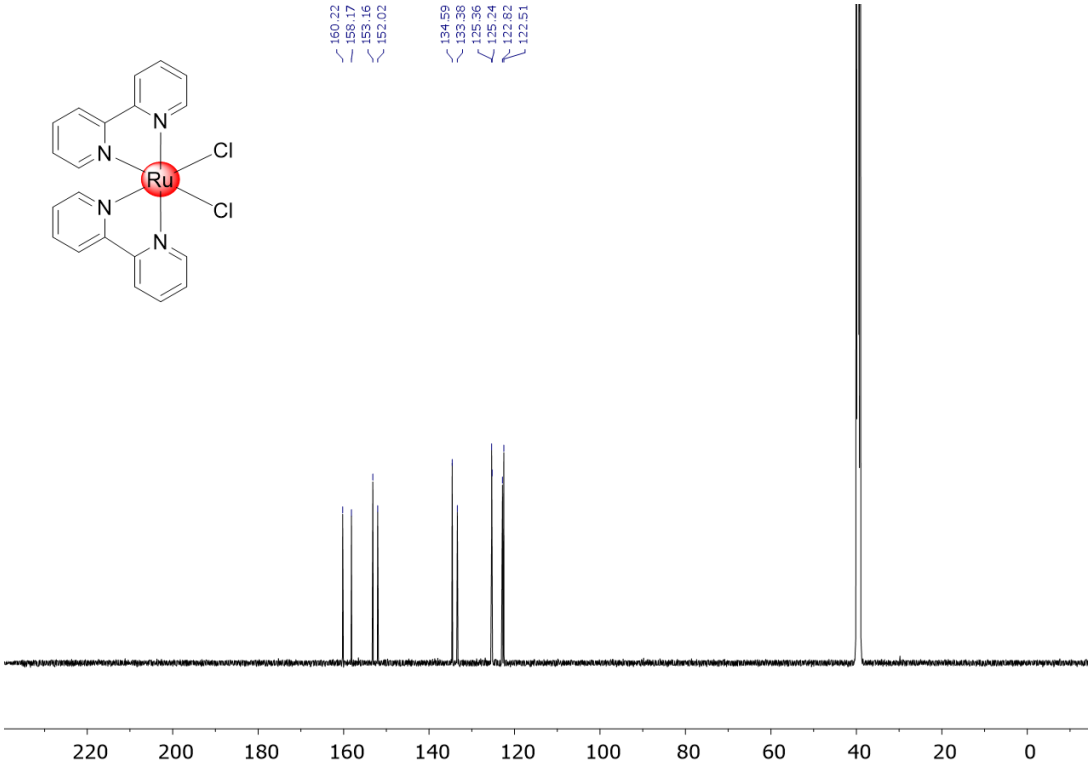

Fig. S12. ^{13}C-NMR (126 MHz, DMSO-d_6) spectrum of [Ru(2,2'-bipyridine)$_2$Cl$_2$].

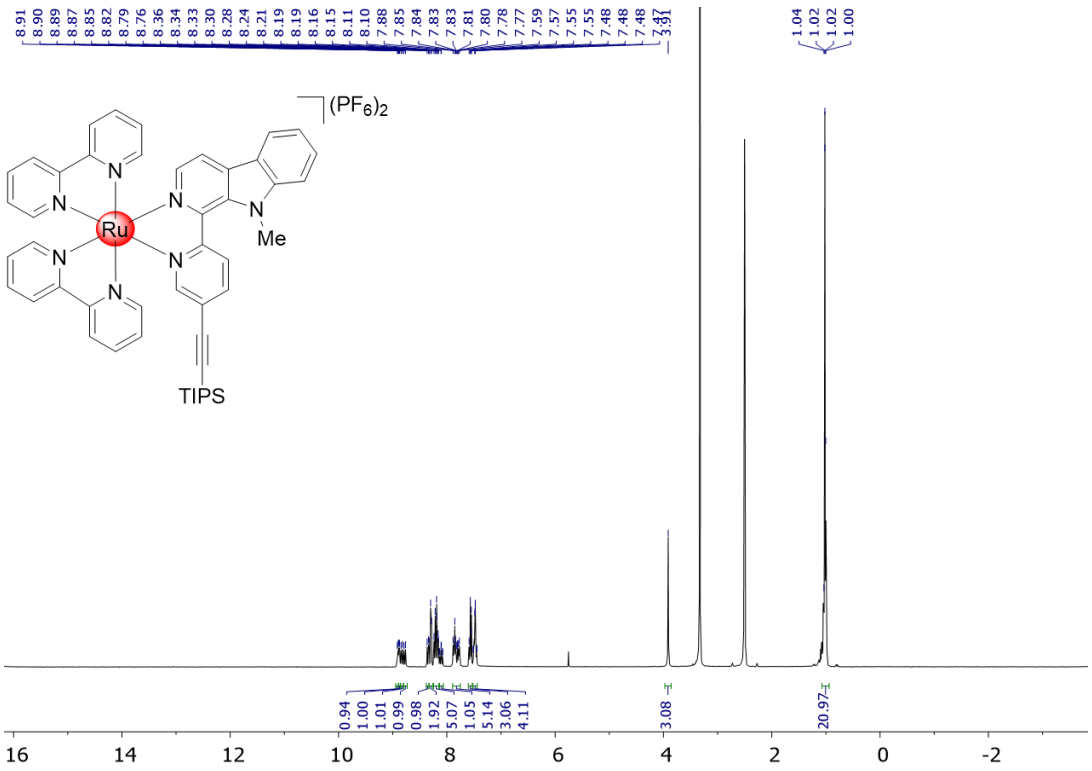

Fig. S13. ^{1}H-NMR (500 MHz, DMSO-d_6) spectrum of [Ru(2,2'-bipyridine)$_2$(9-methyl-1-(5-((triisopropylsilyl)ethynyl)pyridin-2-yl)-β-carboline)][PF$_6$]$_2$.

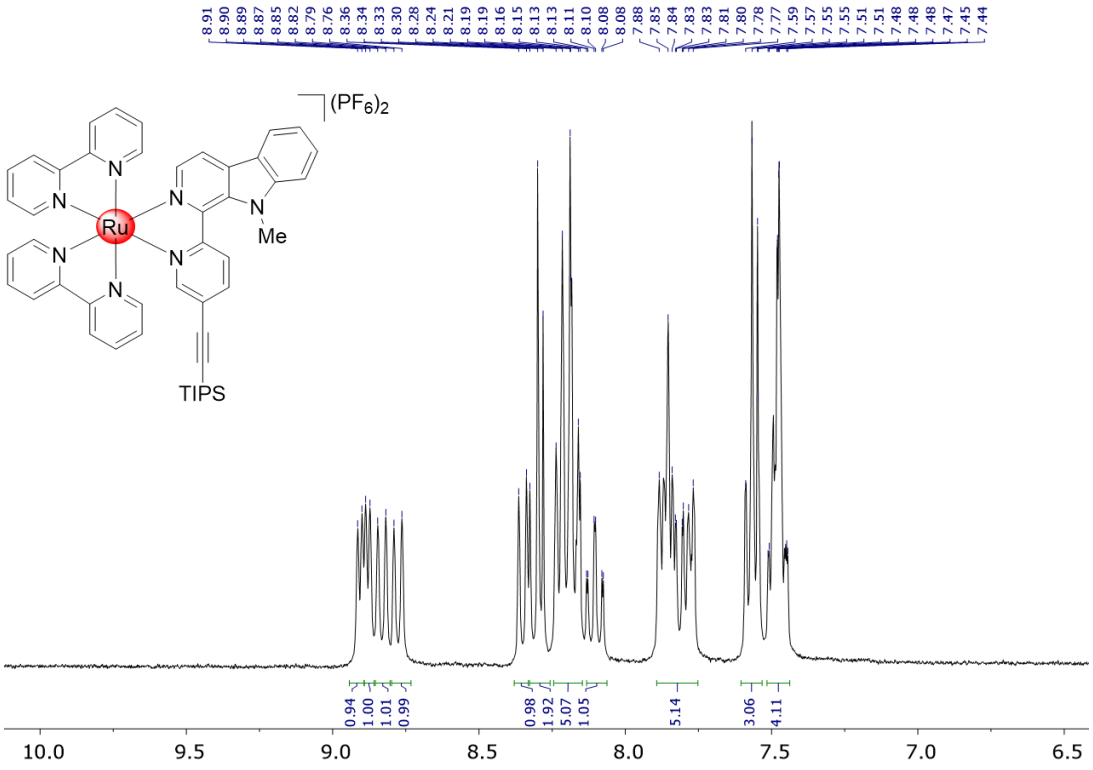

Fig. S14. ^{1}H-NMR (500 MHz, DMSO-d_6) spectrum of [Ru(2,2'-bipyridine)$_2$(9-methyl-1-(5-((triisopropylsilyl)ethynyl)pyridin-2-yl)-β-carboline)][PF_6]$_2$ in the aromatic region.

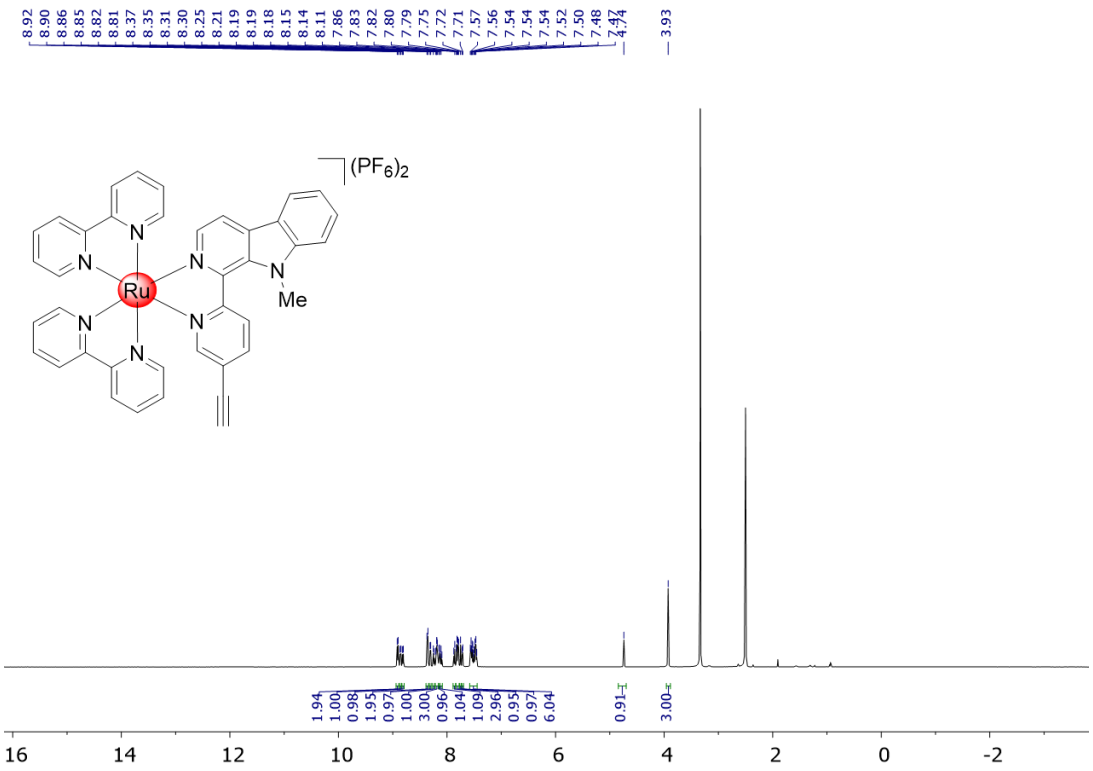

Fig. S15. ^{1}H-NMR (500 MHz, DMSO-d_6) spectrum of [Ru(2,2'-bipyridine)$_2$(1-(5-ethynylpyridin-2-yl)-9-methyl-β-carboline][PF_6]$_2$.

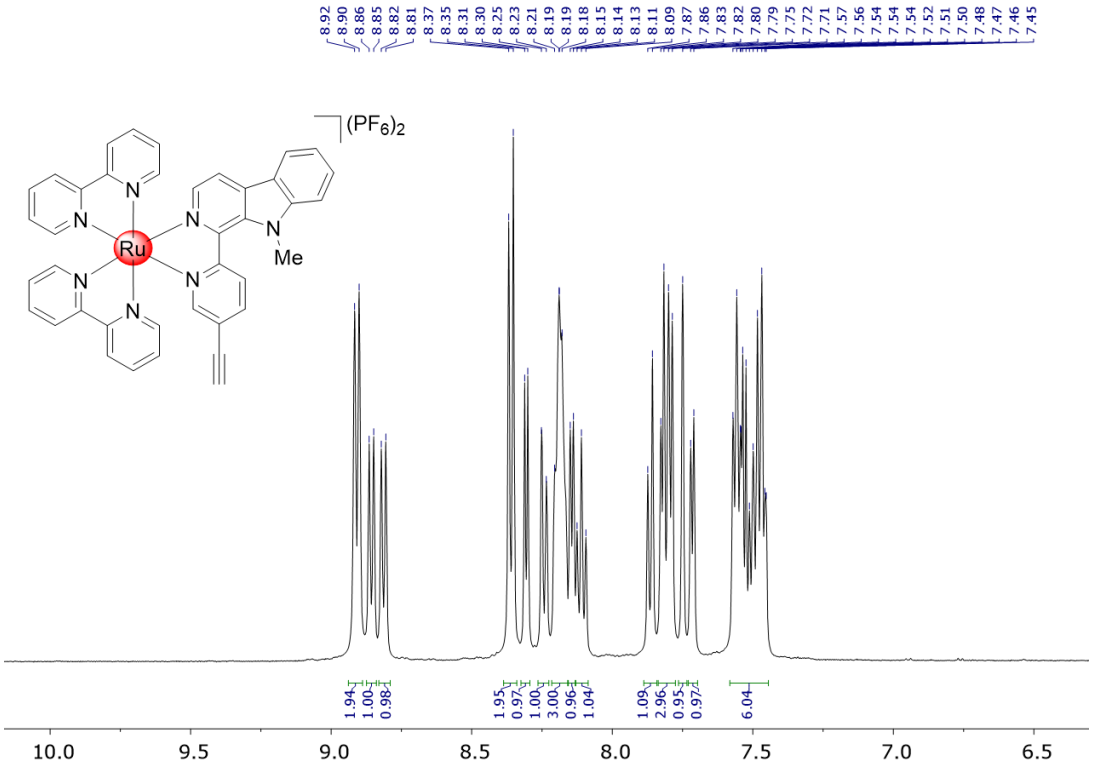

Fig. S16. ^{1}H-NMR (500 MHz, DMSO-d_6) spectrum of [Ru(2,2'-bipyridine)$_2$(1-(5-ethynylpyridin-2-yl)-9-methyl-β-carboline][PF_6]$_2$ in the aromatic region.

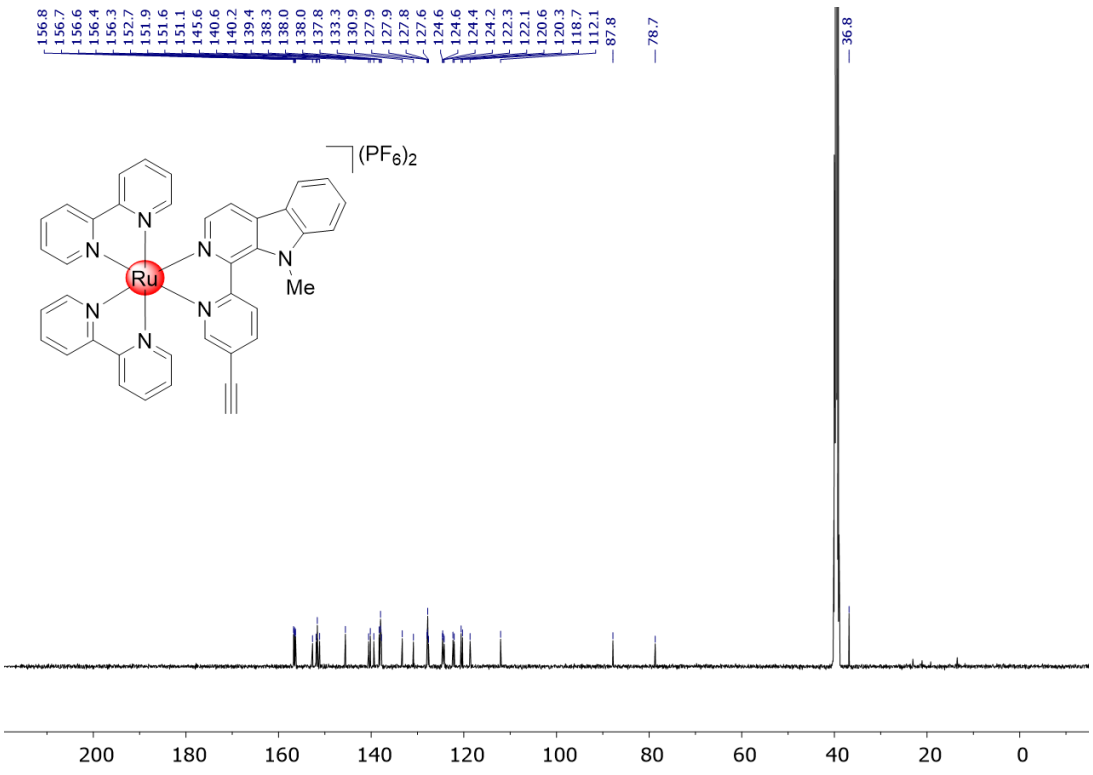

Fig. S17. ^{13}C-NMR (126 MHz, DMSO-d_6) spectrum of [Ru(2,2'-bipyridine)$_2$(1-(5-ethynylpyridin-2-yl)-9-methyl-β-carboline][PF_6]$_2$.

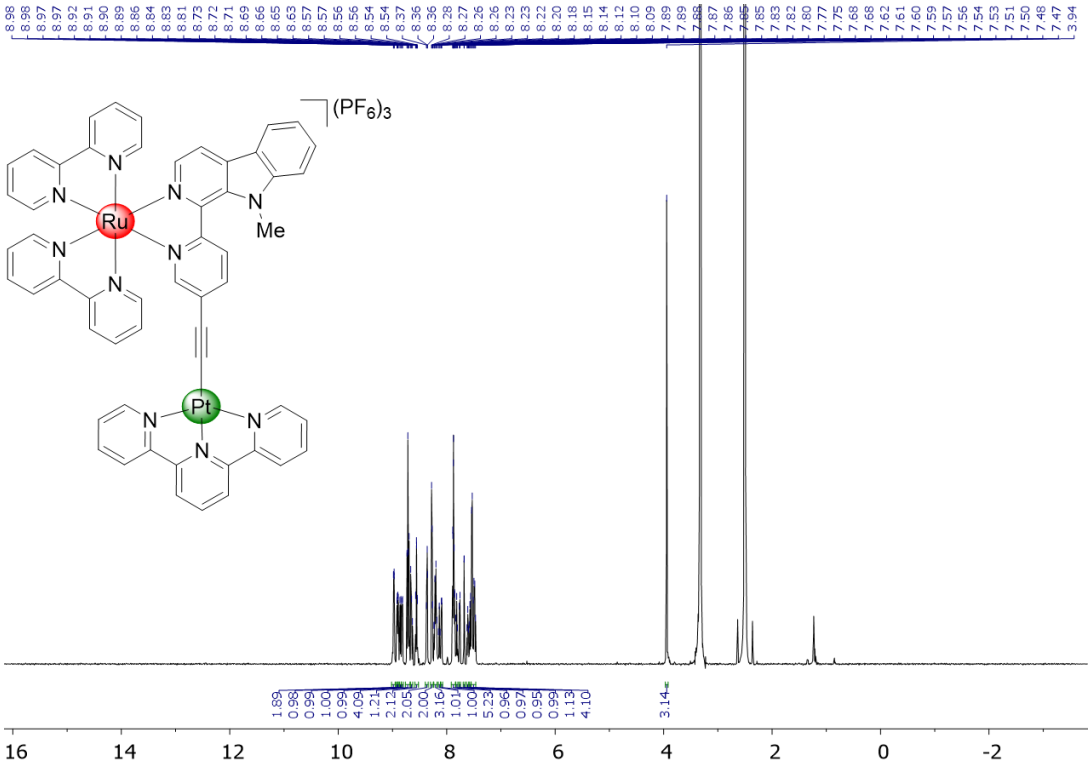

Fig. S18. ^{1}H-NMR (500 MHz, DMSO-d$_6$) spectrum of **RuPt**.

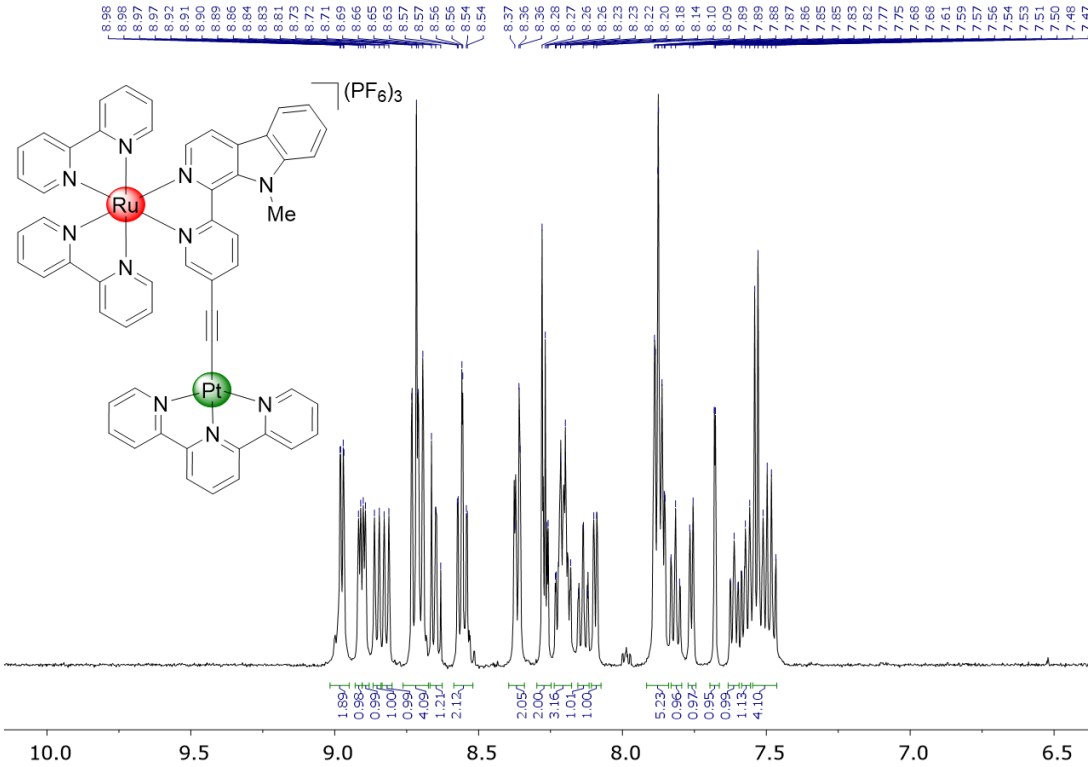

Fig. S19. ^{1}H-NMR (500 MHz, DMSO-d$_6$) spectrum of **RuPt** in the aromatic region.

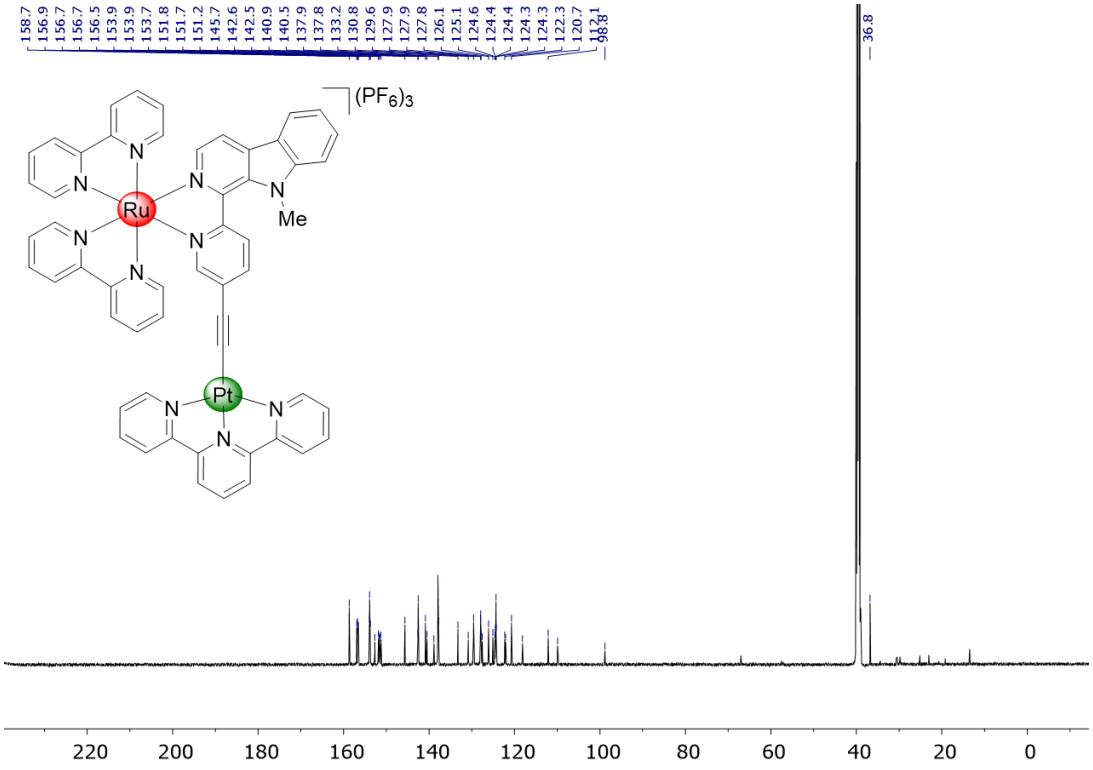

Fig. S20. ^{13}C-NMR (126 MHz, DMSO-d_6) spectrum of **RuPt**.

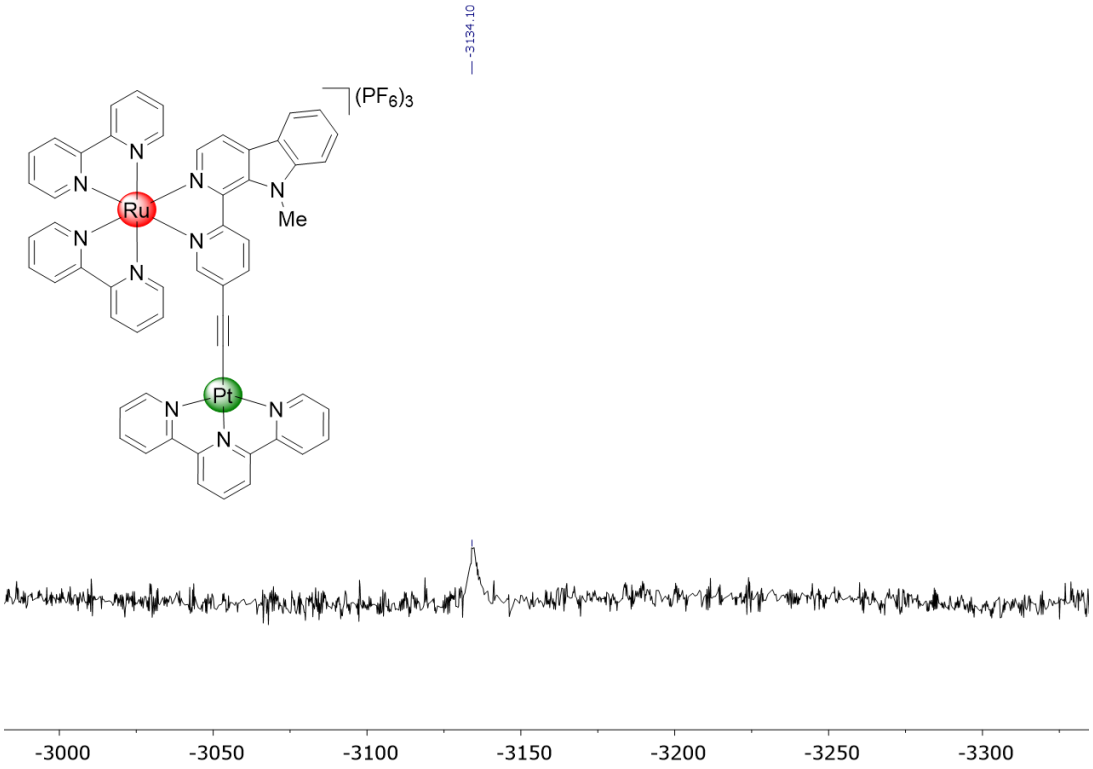

Fig. S21. ^{195}Pt-NMR (107 MHz, DMSO-d_6) spectrum of **RuPt**.

2.3 ESI Data

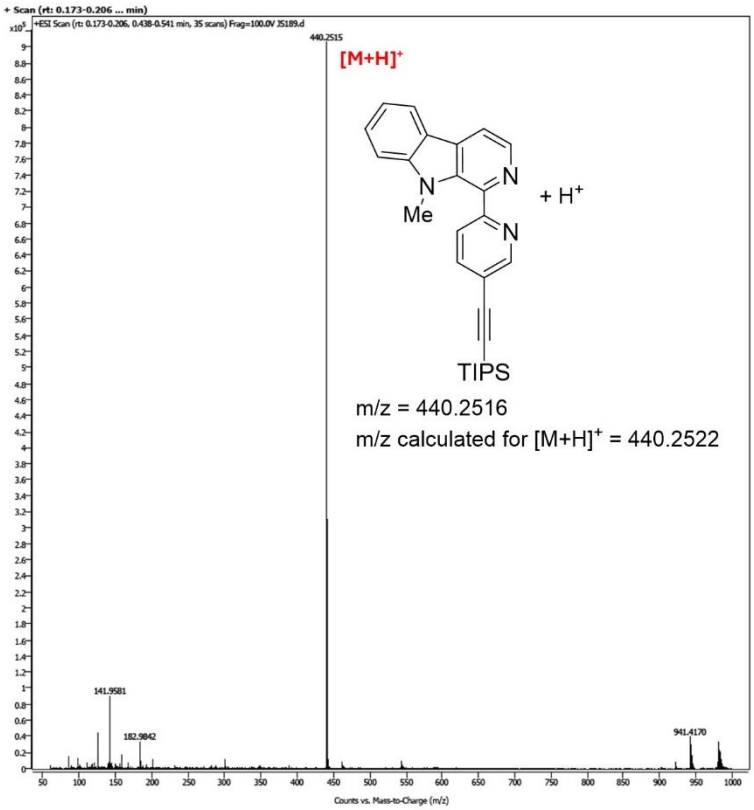

Fig. S22. HR-ESI(+) mass spectrum of 9-methyl-1-(5-((triisopropylsilyl)ethynyl)pyridin-2-yl)-β-carboline.

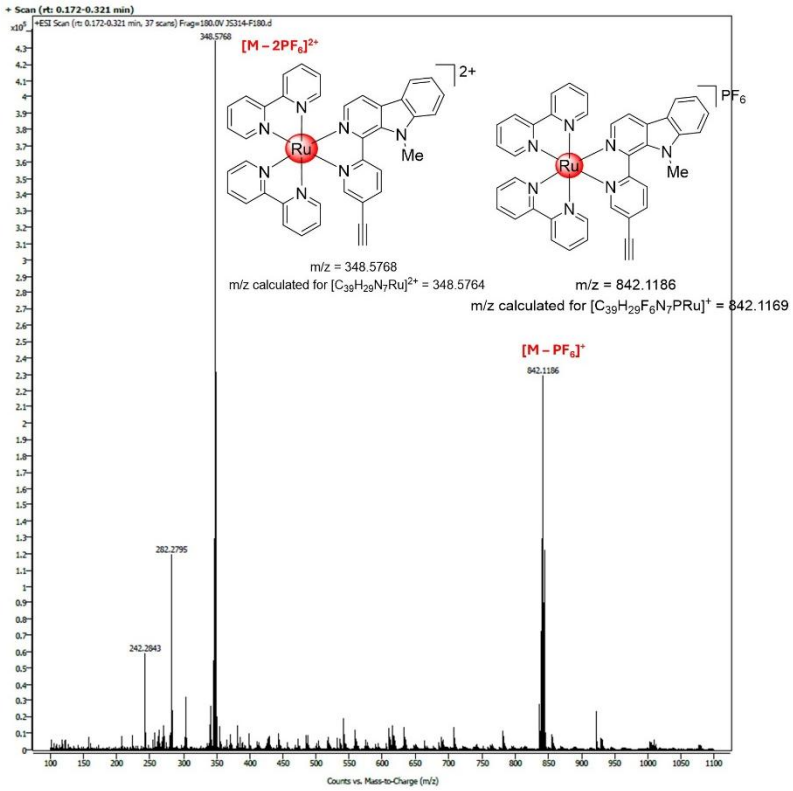

Fig. S23. HR-ESI(+) mass spectrum of complex [Ru(2,2'-bipyridine)$_2$(1-(5-ethynylpyridin-2-yl)-9-methyl-β-carboline][PF_6]$_2$.

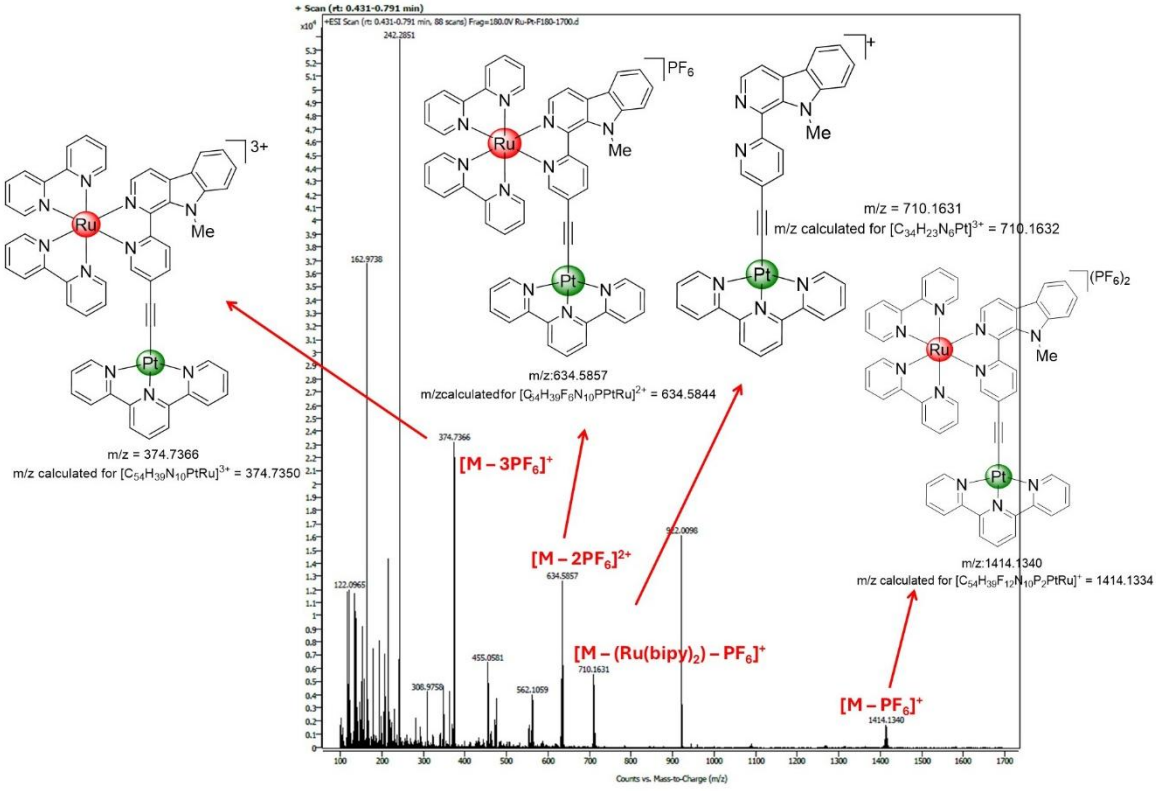

Fig. S24. HR-ESI(+) mass spectrum of complex **RuPt**.

3. Fabrication of Membranes

3.1 General procedure

For membrane fabrication, the RuPt derivative was first dissolved in an appropriate solvent system (DMF or DMF/THF mixture). After complete dissolution of the complex, either poly(ε-caprolactone) (PCL, Mw = 80,000, Sigma-Aldrich, Germany) or polyacrylonitrile (PAN, Mw = 150,000, Sigma-Aldrich, Germany) was added to the solution and stirred until a homogeneous spinning solution was obtained.

The resulting solution was transferred into a 5 mL syringe equipped with a 20G needle and processed by electrospinning. Fiber formation was carried out using a horizontally configured electrospinning setup with a rotating metallic drum collector operating at 315 rpm. The process was conducted under controlled environmental conditions at 20–25 °C and a relative humidity of 30–40%. The obtained electrospun membrane was A4-sized and homogeneous across the entire surface. For subsequent analyses, samples of identical dimensions were punched from the membranes using a standardized round punch, ensuring consistent sample geometry and comparability across all further studies.

The electrospinning parameters used for membrane fabrication are summarized in Table below.

Membrane	**Polymer /PS w/w**	**solvent**	**ratio**	**ml/h**	**Voltage [kV]**	**TOC /cm**
PCL-RuPt	15	THF/DMF	1:1	1.20	20	15.0
PAN-RuPt	10	DMF	1	3.00	25	10.0

THF – tetrahydrofuran, DMF – dimethylformamide.

3.2 Characterization through SEM

The morphology of the electrospun membranes was characterized by scanning electron microscopy (SEM) using an Apreo S LoVac system (Thermo Fisher Scientific, Waltham, MA, USA). Prior to imaging, the samples were fixed onto conductive carbon adhesive tape and coated with a thin Au/Pd layer to ensure sufficient surface conductivity. Images were recorded at magnifications of 1000x, 5000x, and 20,000x. Fiber diameter analysis was performed using ImageJ software, with measurements taken at more than 100 randomly selected locations to ensure statistical relevance.

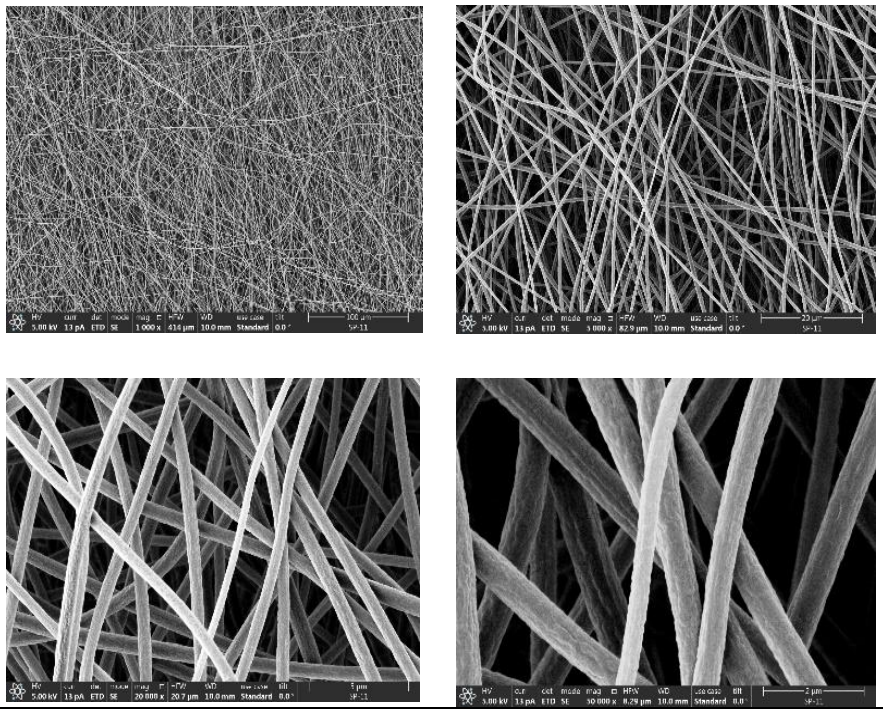

PAN-RuPt

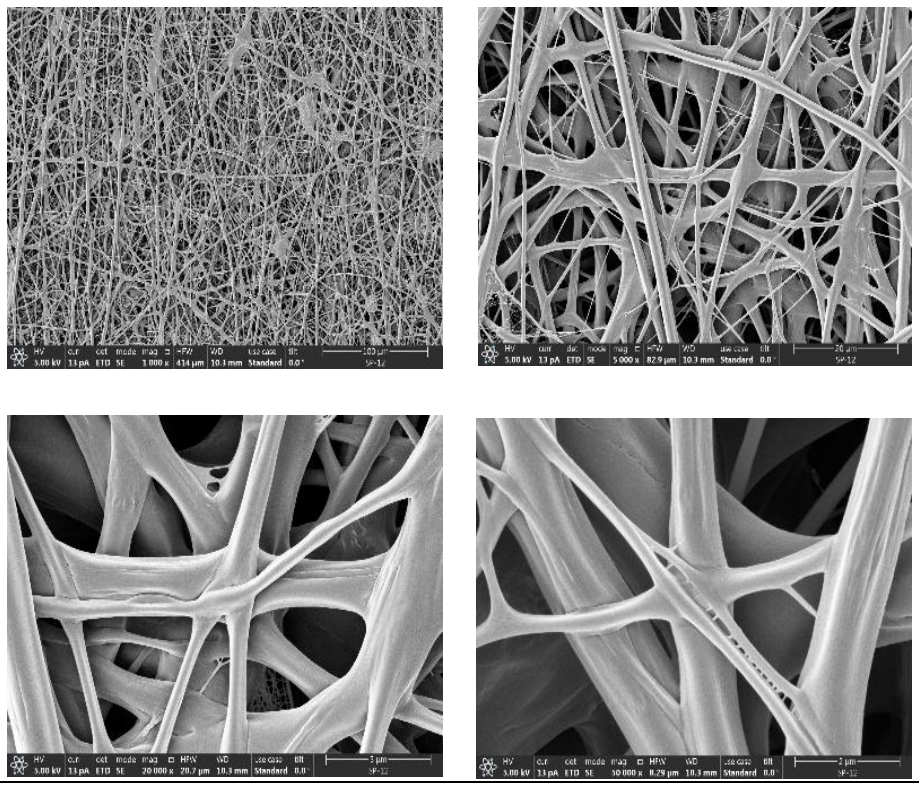

PCL-RuPt

Fig. S25. SEM images of all membranes used in this study for analysis of the surface morphology.

3.3 Water contact angle measurements

Water contact angle measurements were carried out to evaluate the surface wettability of the electrospun membranes containing the RuPt complex. The measurements were performed using the sessile drop method at room temperature with deionized water as the probe liquid. For each membrane, four independent measurements were conducted. The temporal evolution of the water contact angle was recorded after droplet deposition. For clarity, one representative set of time-dependent contact angle images is presented for each membrane, while the reported contact angle values correspond to the average of four measurements.

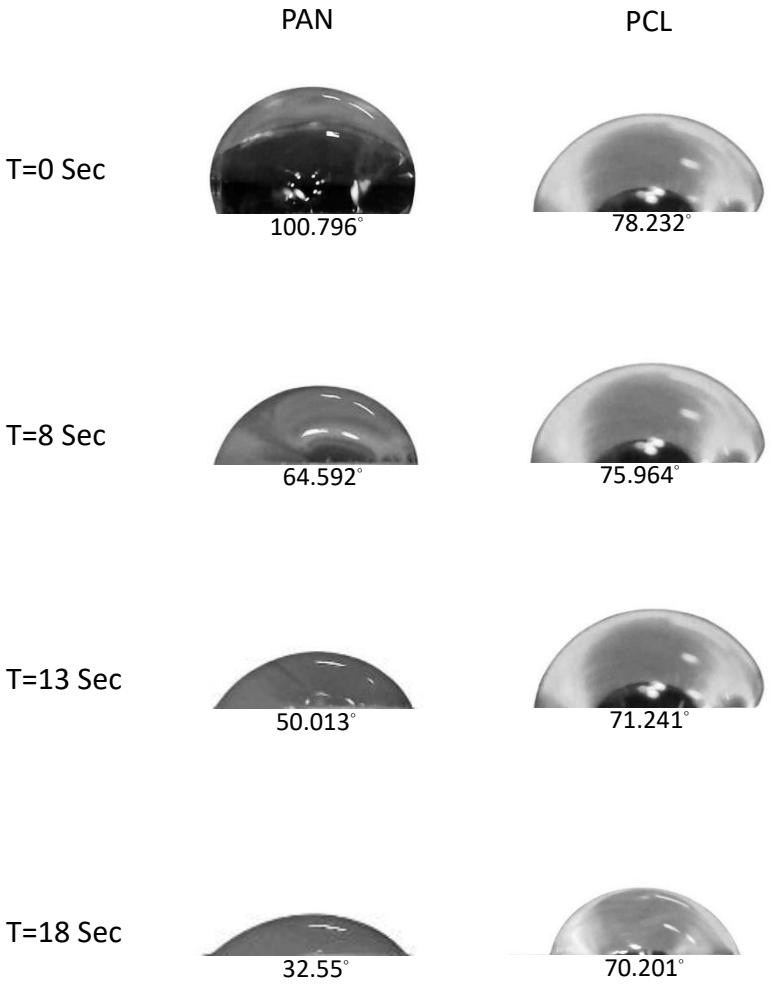

Fig. S26. Water contact angle of all membranes used in this study.

4. Photophysical Characterization

4.1 UV-Vis Absorption and Photoluminescence Spectra

UV-Vis absorption spectra were recorded on a Jasco V-750 UV-Visible spectrophotometer while excitation and emission spectra were recorded on a FLS980 spectrofluorometer (from Edinburgh Instruments) equipped with triple grating turret monochromators and a Red PMT Sphere detector. The F980 spectrometer operating software was used to collect and process fluorescence data. For the fluorescence measurements, samples of 10^{-5} M solutions in water:dimethyl sulfoxide (99:1) were prepared and deoxygenated in a Schlenk flask using Freeze-Pump-Thaw technique and transferred, under inert atmosphere, into 10 mm quartz cells equipped with Teflon septum. The luminescence emission spectra were excited at 450 nm with a Xenon Arc lamp and the maximum emission wavelength was recorded from 500 to 800 nm. The photoluminescence quantum yields (PLQY) were calculated by using an integrating sphere. For the determination of the luminescence lifetime, the fluorescence decay was measured on a FLS980 spectrofluorometer equipped with a TSCPC laser (λ_{ex} = 450 nm) and a REDPMT detector.

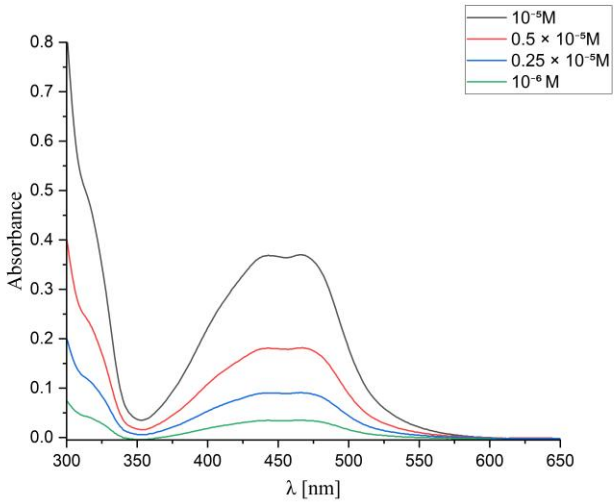

Fig. S27. UV-Vis spectra of **RuPt** used in this study in DMF at different concentrations from 1 μM to 10 μM.

4.2 Singlet Oxygen measurements by indirect method in H_2O and DMSO

The efficiency of RuPt to generate singlet oxygen ($^1O_2$) was experimentally determined indirectly in our previous work by using 9,10-anthracenediyl-bis(methylene) dimalonic acid (ABDA).[1] In summary, aerated solutions containing ABDA (8×10^{-5} M) and the corresponding photosensitizer in water:dimethyl sulfoxide (99:1) were exposed to blue LED light irradiation (λ_{irr} = 460 nm; 24 W) at room temperature for irradiation intervals of 5 minutes for monometallic complexes (0 min→30 min) and 2.5 minutes for the heterobimetallic complex (0 min→15 min). The corresponding UV-Vis spectrum was recorded after every irradiation interval. Concentrations of metal complexes were tuned to achieve similar values of absorbance at 460 nm ($A_{460\ nm} \approx 0.06$). The singlet oxygen quantum yield was determined using $[Ru(bipy)_3]Cl_2$ as reference ($\Phi_\Delta = 0.18$ in water) and the following equation:

$$\Phi_{PS} = \Phi_{ref} \times \frac{k_{PS}}{k_{ref}} \times \frac{A_{ref}}{A_{PS}}$$

k_{PS} and k_{ref} represent the decomposition rate constants of the photobleaching of ABDA for the evaluated photosensitizer and reference, respectively. The constants were determined by the slope calculated from the linear fit of $\ln(A_0/A)$ vs time. A_0 corresponds to the absorbance of ABDA at 378 nm before irradiation, while A is the ABDA absorbance at 378 nm at different irradiation times. A_{ref} and A_{PS} correspond to absorbance at 460 nm of $[Ru(bipy)_3]Cl_2$ and the PS respectively. Φ_{ref} is the singlet-oxygen quantum yield of $[Ru(bipy)_3]Cl_2$ (Φ_{ref} = 0.18 in water).

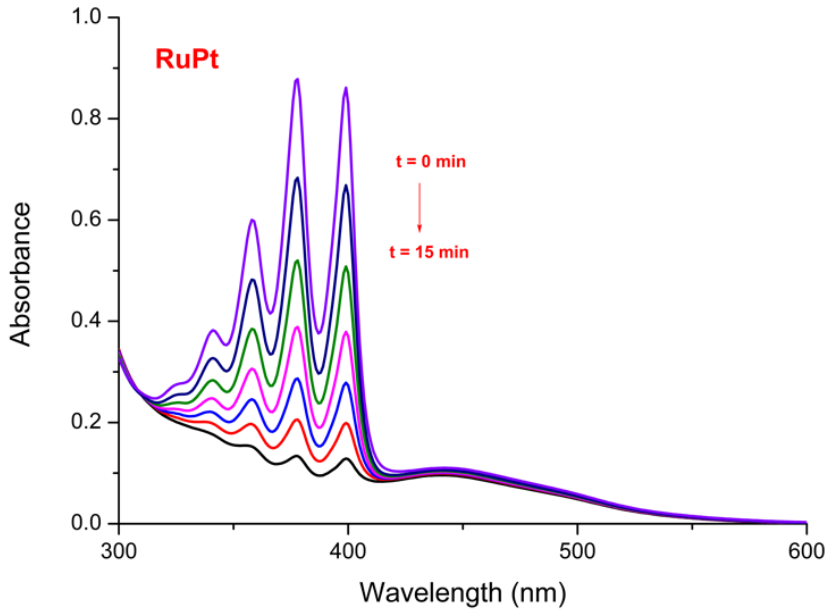

Fig. S28. Absorbance spectra of ABDA upon irradiation in the presence of **RuPt**. Data retrieved with permission from *Sanz-Villafruela* et al, Inorg. Chem. Front., 2025,12, 5770-5782 under a CC-BY *3*.0 license.

4.3 Singlet Oxygen measurements by direct method in ACN

The singlet oxygen quantum yield (ΦΔ) of the photosensitizer was determined in acetonitrile (ACN) using a relative method. Tris(2,2′-bipyridyl)dichlororuthenium(II) hexahydrate (Φ_Δ = 0.57 in ACN) was employed as a reference compound.

Upon photoexcitation, the near-infrared emission arising from singlet oxygen phosphorescence was recorded. The integrated emission intensity of the $^1O_2$ phosphorescence signal was determined for both the reference and the sample and used to calculate Φ_Δ.

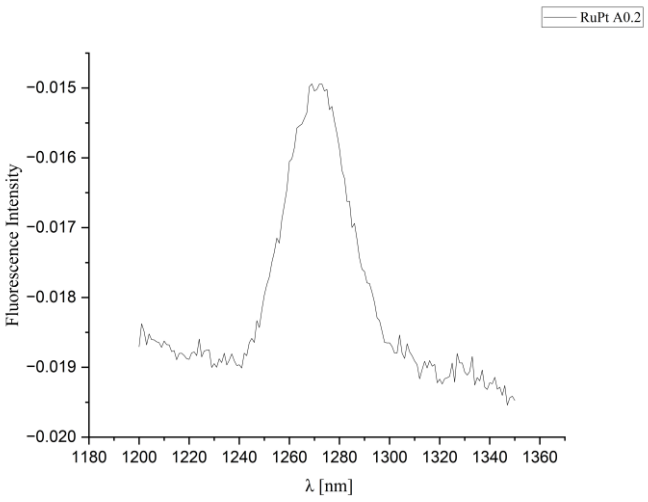

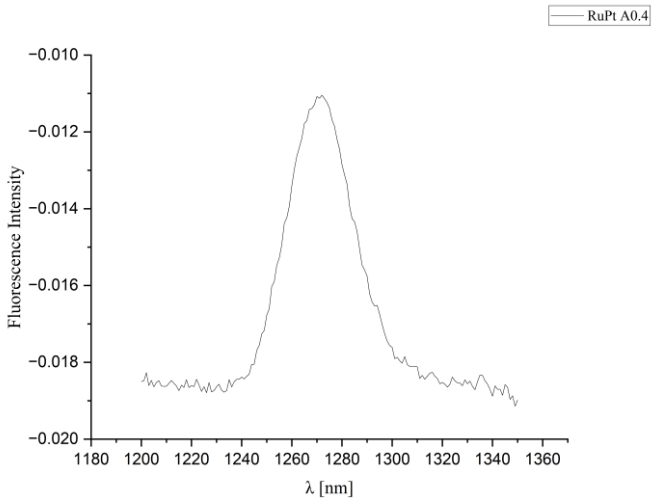

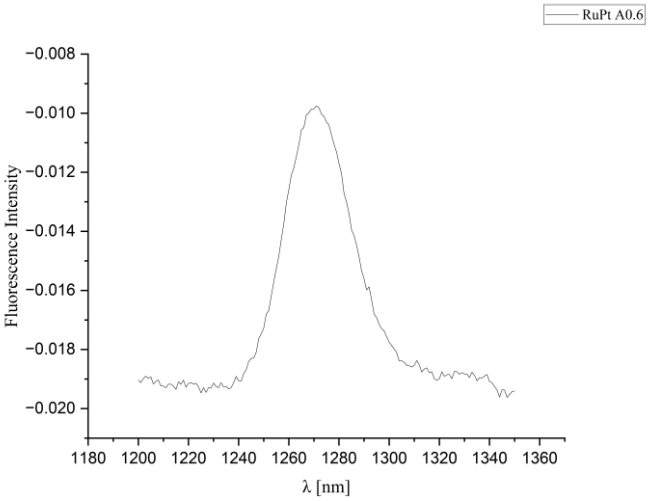

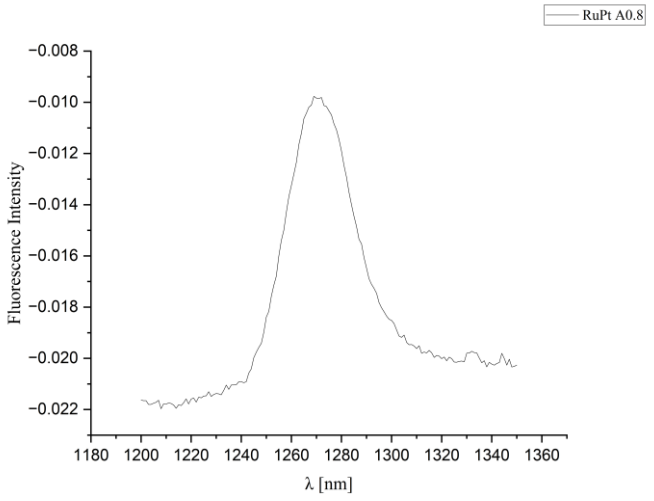

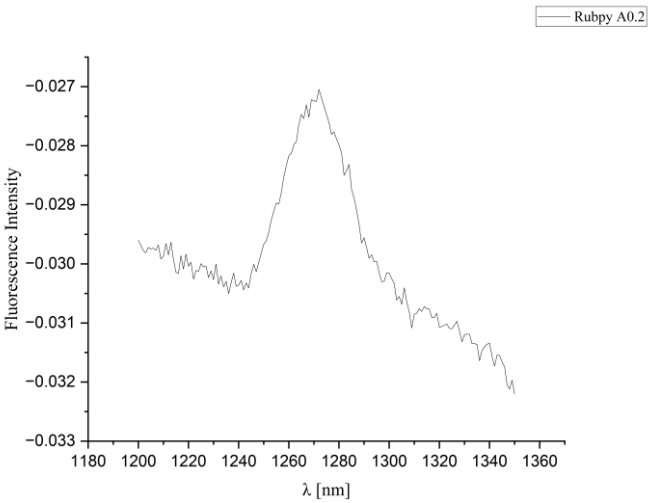

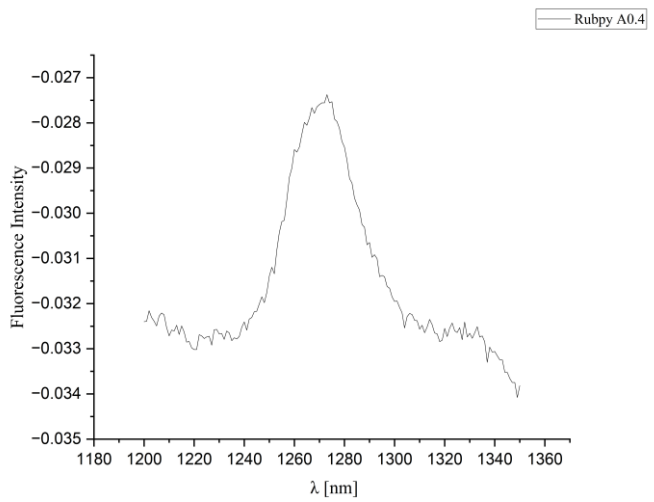

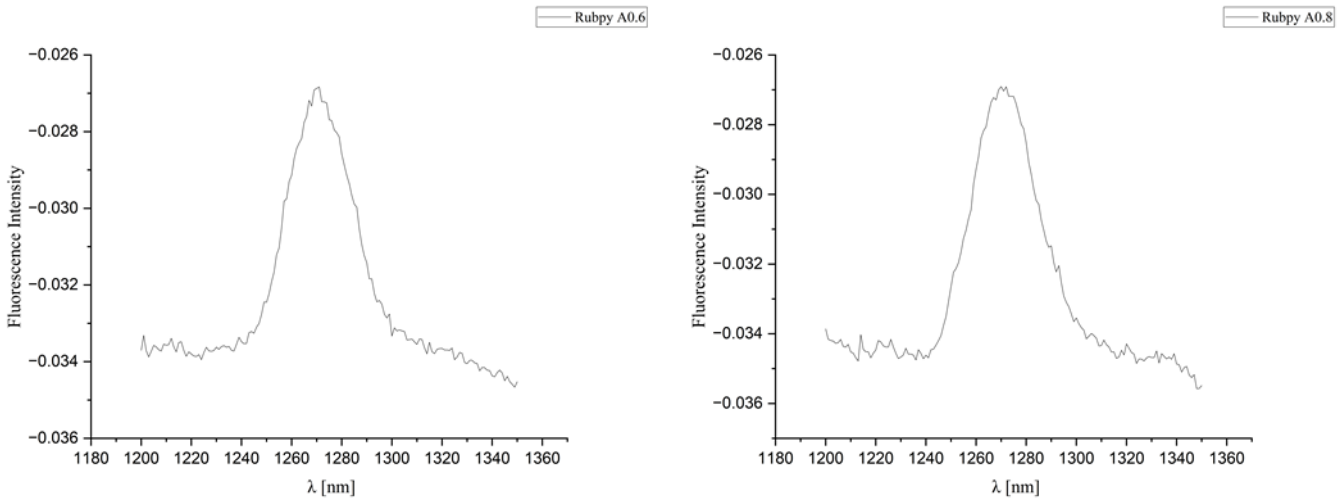

Fig. S29. $^1O_2$ emission spectra of **RuPt** and **Rubpy** upon photoexcitation in ACN.

Measurement I

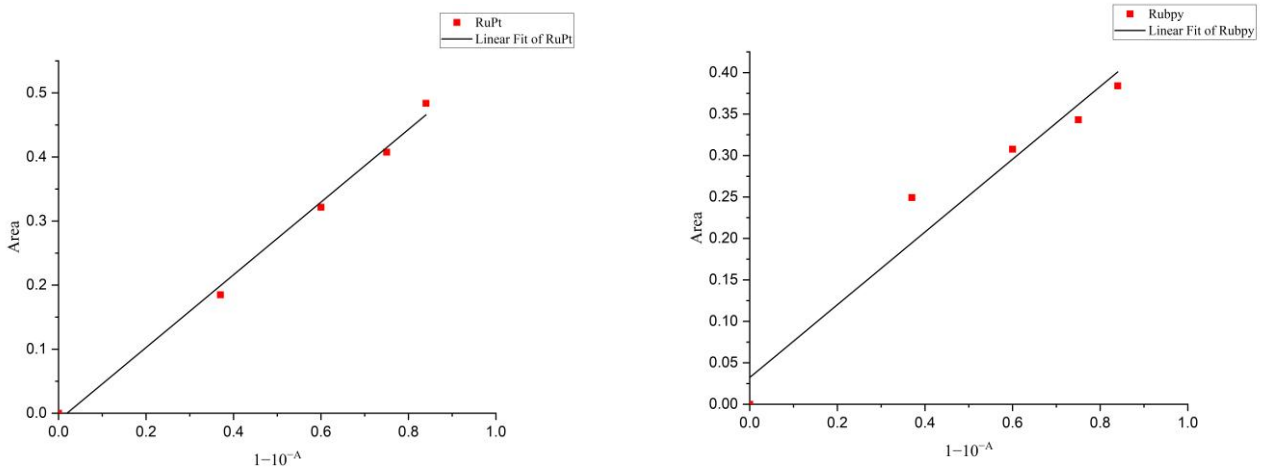

Measurement II

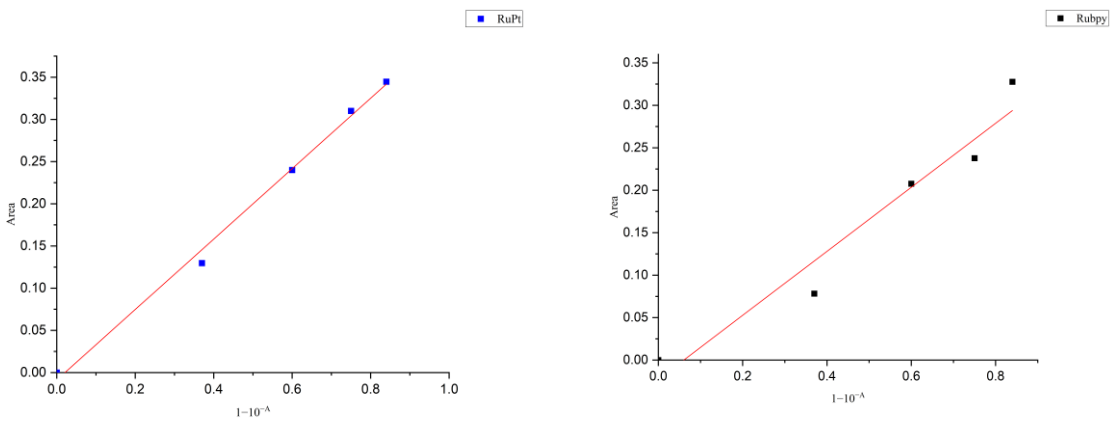

Measurement III

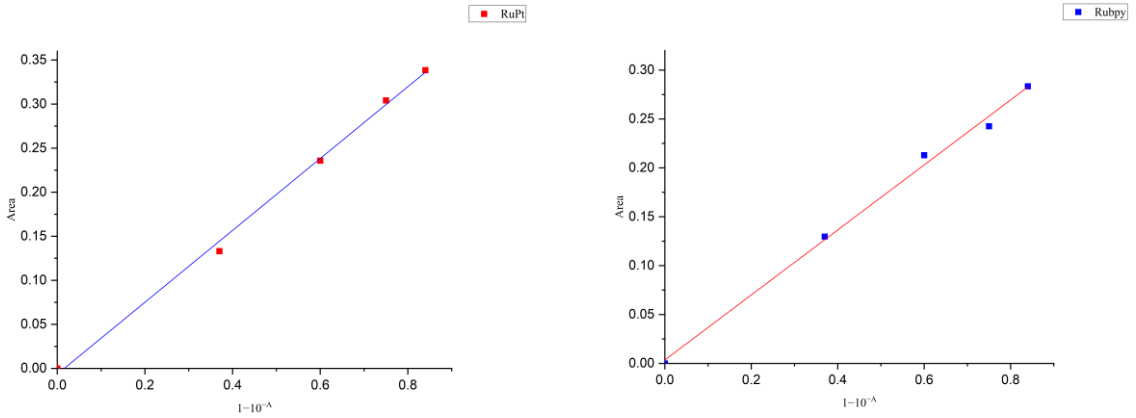

Fig. S30. Fraction of light absorption vs. Area plot for **RuPt** and **Rubpy**.

4.4 Detection of Superoxide Radical (•O_2^-) Using Dihydroethidium (DHE)

Superoxide radical ($^{\bullet}O_2^-$) generation was evaluated using dihydroethidium (DHE) as a fluorescent probe. DHE was used at a final concentration of 50 µM in the presence of calf thymus DNA (ctDNA, 250 µg/mL). The solution was irradiated in the presence of the RuPt complex. Upon reaction with $^{\bullet}O_2^-$, DHE is oxidized to ethidium, which intercalates into DNA and exhibits fluorescence emission centered at 577 nm. The increase in fluorescence intensity at 577 nm was monitored over time and used as an indicator of superoxide generation.

Measurement I

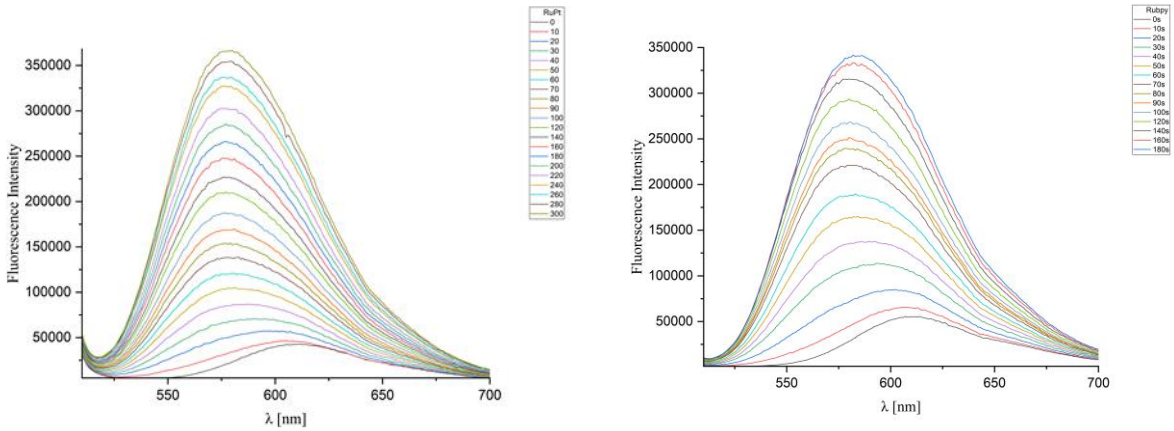

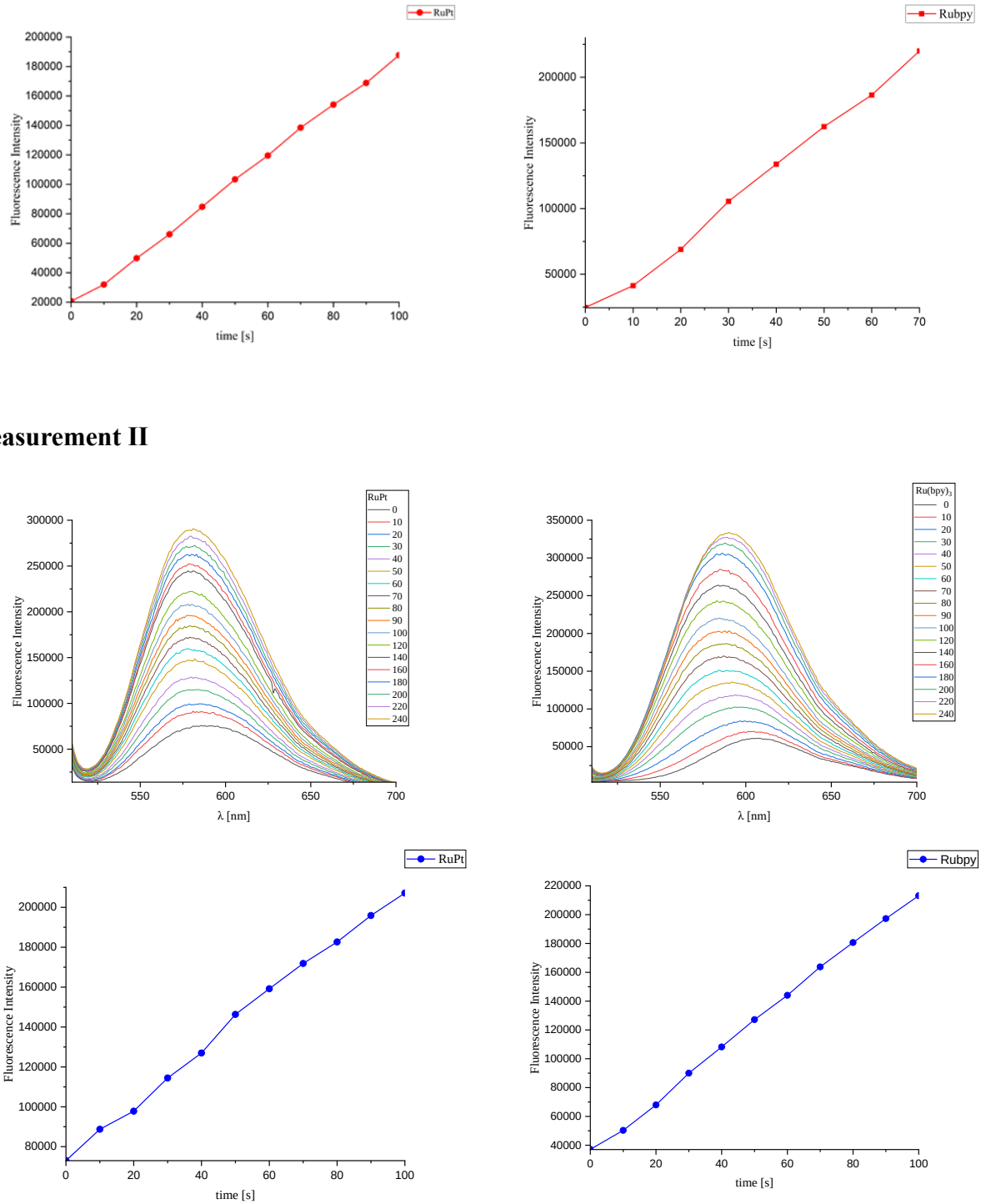

Fig. S31. Detection of superoxide radical ($\bullet O_2^-$) using DHE. Top: Time-dependent fluorescence emission spectra of DHE in the presence of ctDNA upon irradiation of RuPt (left) and Tris(2,2′-bipyridyl)ruthenium(II) chloride (right) under identical conditions for two measurements. Bottom: Corresponding plots of fluorescence intensity at 577 nm vs. irradiation time.

4.5 Stability

The stability of RuPt was evaluated in our previous work.[1] In summary, a solution containing the metal complex (10^{-5} M) in phosphate-buffered saline:dimethyl sulfoxide (99:1) was monitored by UV-Vis. The absoprtion spectra were recorded at different periods of time (0, 24 and 48 h) at room temperature. A reduction in the absorbance at the local maxima located around 425 nm was used to evaluate their photostability. No significant changes were observed after 48 hours.

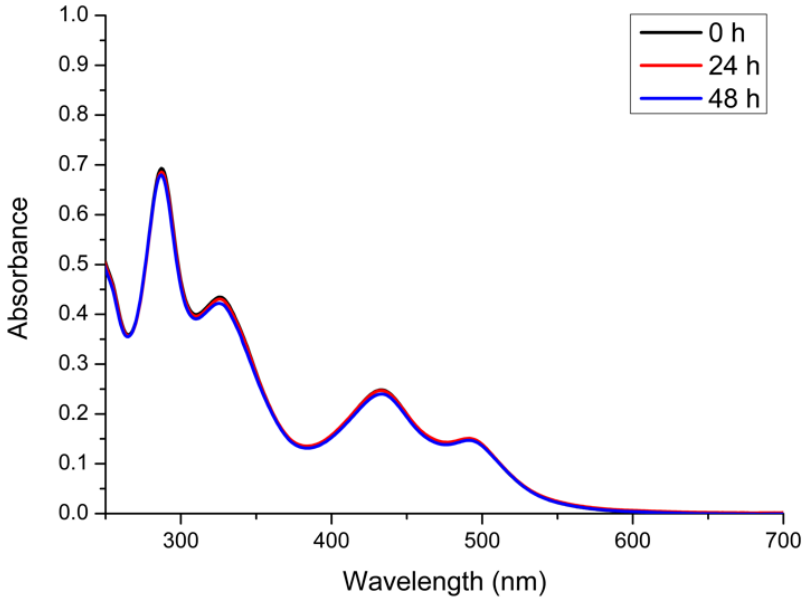

Fig. S32. Stability of **RuPt** (10^{-5} M) in PBS:DMSO (99:1) in dark conditions (0, 24, and 48 h) at room temperature. Data retrieved with permission from Sanz-Villafruela et al, Inorg. Chem. Front., 2025,12, 5770-5782 under a CC-BY 3.0 license.

4.6 (Photo-)Stability

The photostability of RuPt was evaluated by UV-vis in our previous work.[1] In summary, a 10^{-5} M solution in water:dimethyl sulfoxide (99:1) were exposed to blue LED light irradiation (λ_{irr} = 460 nm; 24 W) and spectra were recorded at different periods of time (0, 1, 2, 4 and 6 h) at room temperature. A reduction in the absorbance at the local maxima located around 425 nm was used to evaluate their photostability. The photodegradation of the heterobimetallic complex after 6 h of irrdation (approx. 2%) was calculated considering the reduction in the absorbance at the local maxmium located at 429 nm.

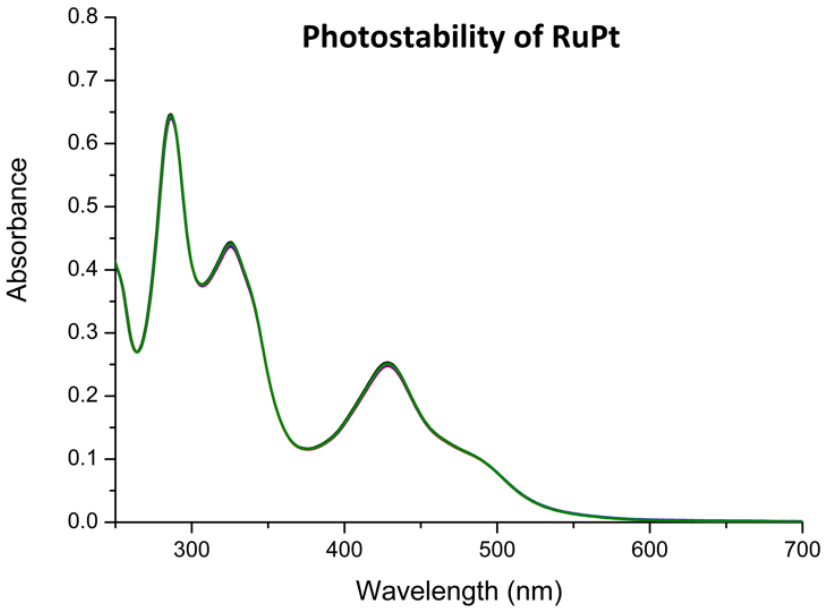

Fig. S33. (Photo-)Stability of **RuPt** in H_2O:DMSO (99:1, v:v) (10^{-5} M) at different times (0, 1, 2, 4, and 6 h) under blue LED light irradiation (460 nm, 24 W) at room temperature. Data retrieved with permission from Sanz-Villafruela et al, Inorg. Chem. Front., 2025,12, 5770-5782 under a CC-BY 3.0 license

4.7 Loading Efficiency

Loading efficiencies were calculated using UV–vis spectroscopy data obtained from membrane samples dissolved in 1.0 mL DMF. Concentrations were calculated using the calibration curve.

Parameters Used
Slope = 37191.4324
Intercept = −0.00276
Molecular weight of RuPt = 1559.0225 $g \cdot mol^{-1}$
Theoretical RuPt loading = 4.47 wt%

Equations Used
$c = (A - b) / m$
$n = c \cdot V$
$m(RuPt) = n \cdot M$
Experimental wt% = [m(RuPt) / membrane mass] × 100
LE (%) = [experimental wt% / theoretical wt%] × 100

PAN–RuPt

Sample	Membrane mass (mg)	Absorbance (466 nm)	LE (%)
1	1.40	0.744	50.0
2	0.83	0.399	45.4
3	0.74	0.430	54.8

Mean ± SD: 50.1 ± 4.7 %

PCL–RuPt

Sample	Membrane mass (mg)	Absorbance (466 nm)	LE (%)
1	1.20	0.621	48.7
2	0.84	0.342	38.5
3	0.65	0.332	48.3

Mean ± SD: 45.2 ± 5.8 %

The loading efficiency of RuPt in the electrospun membranes was determined from three independent membrane samples and is reported as mean ± standard deviation.

4.8 Refractive absorbance spectra of membranes using integrating sphere

Refractive absorbance spectra were measured using a Shimadzu UV-2600i spectrometer equipped with an integrating sphere system. Measurements were carried out following the manufacturer's recommendations using solid samples.

ISR-2600Plus
Integrating Sphere Attachment

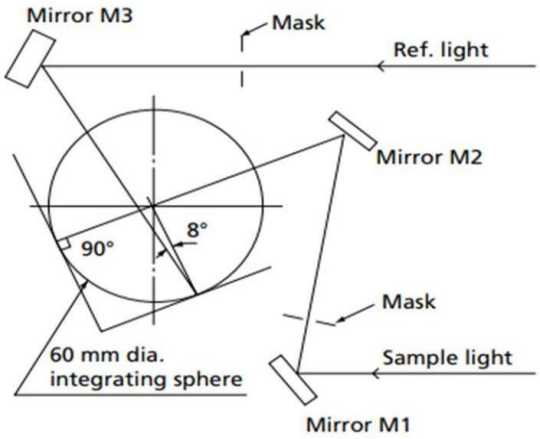

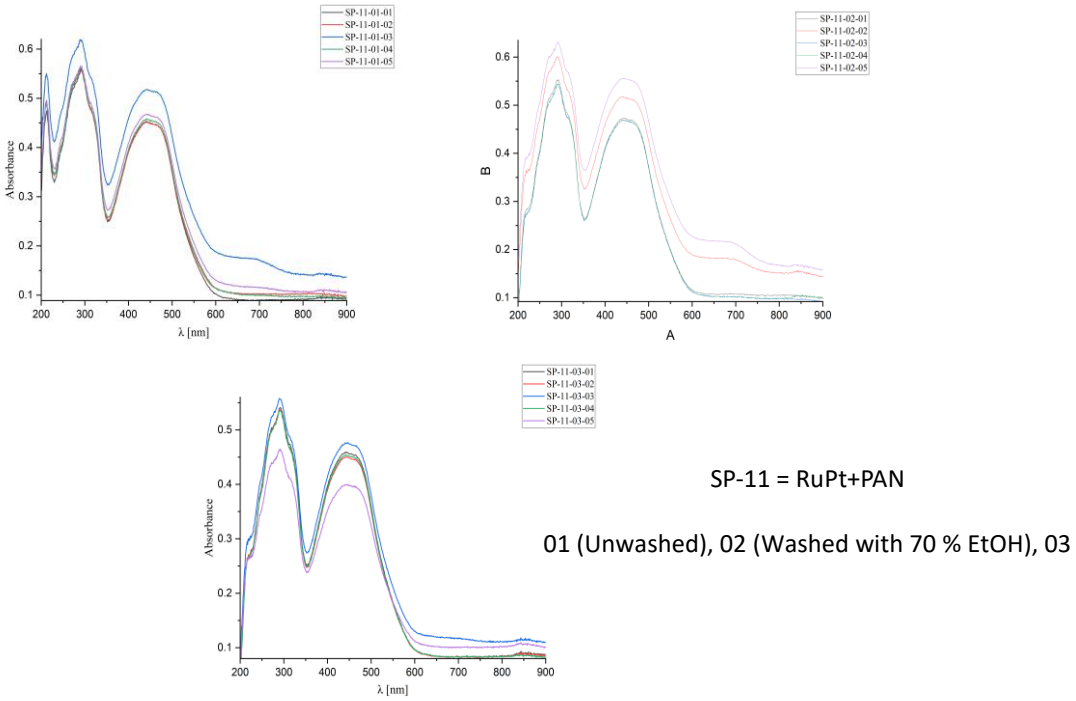

SP-11 = RuPt+PAN

01 (Unwashed), 02 (Washed with 70 % EtOH), 03

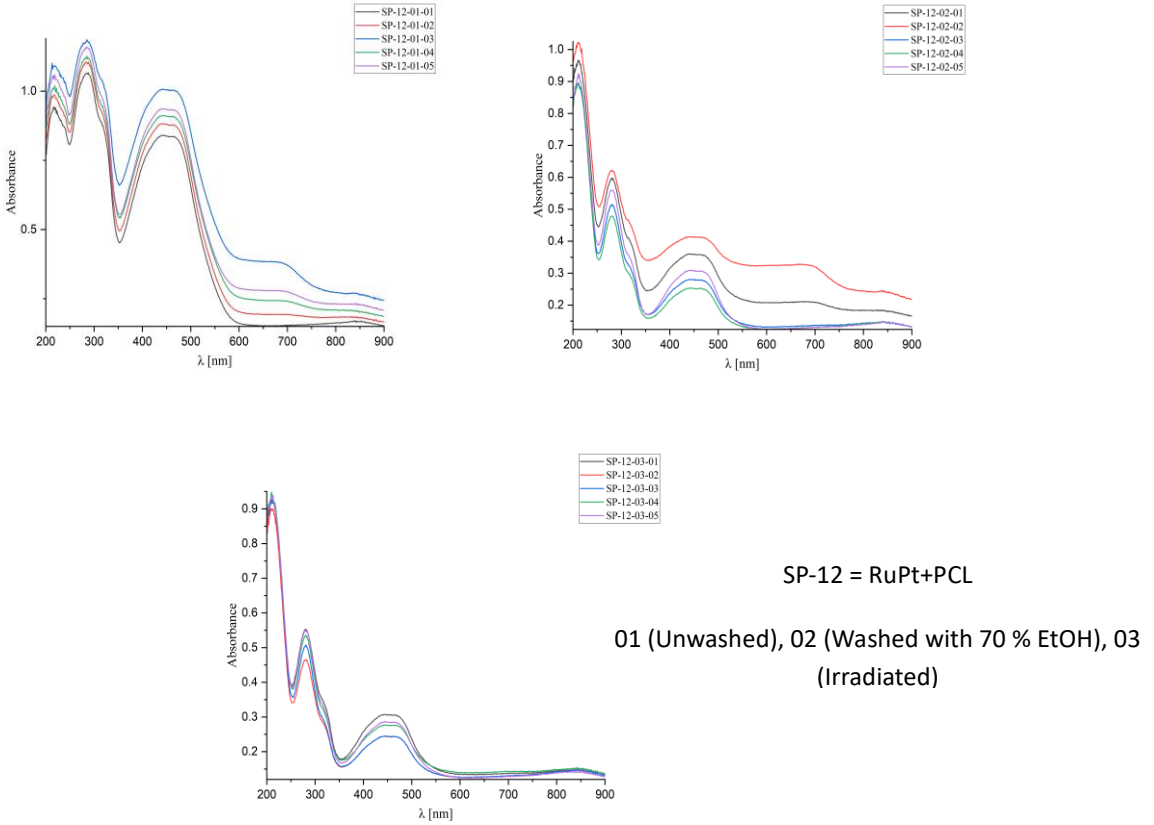

SP-12 = RuPt+PCL

01 (Unwashed), 02 (Washed with 70 % EtOH), 03 (Irradiated)

Fig. S34. Refractive absorbance spectra of membranes used in this study containing **RuPt** as a PS.

4.9 Bleaching Experiments Monitored by Integrating-Sphere UV–Vis Spectroscopy

Membrane discs were prepared, weighed, and subjected to stability analysis. For post-washing evaluation, samples were treated with 70 vol% EtOH for 2 h under exclusion of light, followed by rinsing with H_2O and drying under reduced pressure. All measurements were performed in triplicate.

For photobleaching studies, membranes were irradiated in H_2O with red light for 1 h, dried under reduced pressure, and subsequently dissolved in DMF for quantitative UV–vis analysis ($\lambda = 466$ nm).

The photosensitizer content normalized to membrane mass was calculated according to:

$$C_{xh} = \frac{A \cdot V}{m}$$

where Ais the absorbance of the dissolved membrane, Vthe solution volume, and mthe membrane mass.

The relative loss after irradiation was determined as:

$$L_{1h}(\%) = \left(1 - \frac{C_{1h}}{C_0}\right) \times 100$$

where $C_0$and C_{1h}denote the normalized PS content before and after 1 h of irradiation, respectively.

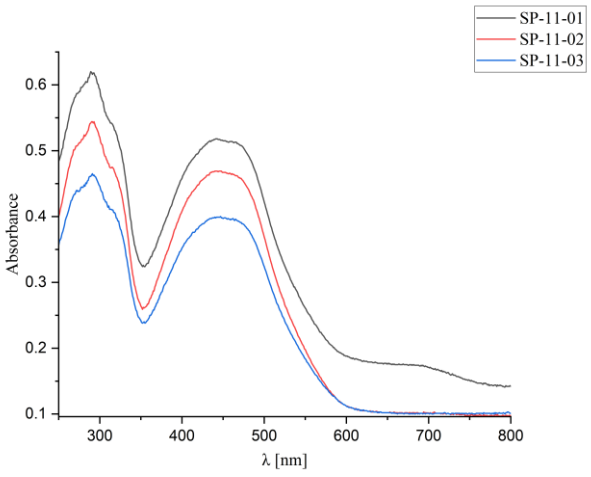

SP-11 = RuPt+PAN

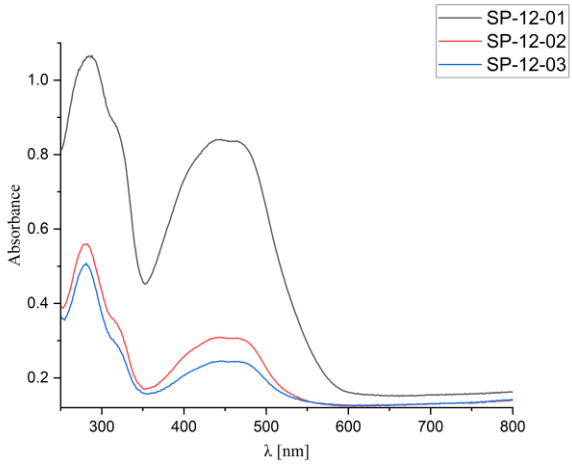

SP-12 = RuPt+PCL

01 (Unwashed), 02 (Washed with 70 % EtOH), 03 (Irradiated)

Loss of RuPt from electrospun membranes after washing with EtOH, determined by integrating-sphere UV–vis spectroscopy:

Membrane	Loss after washing (%)
PAN–RuPt	1.2 ± 9.7
PCL–RuPt	59.9 ± 14.9

RuPt is strongly retained in PAN

~60% loss already after washing, for PCL–RuPt

After washing with EtOH, PAN–RuPt membranes showed no measurable RuPt loss, whereas PCL–RuPt membranes exhibited substantial leaching (~60%), indicating weaker retention of RuPt in the PCL matrix.

Loss of RuPt from electrospun membranes after irradiation, determined by integrating-sphere UV–vis measurements:

Membrane	Loss after irradiation (%)
PAN–RuPt	11.7 ± 9.5
PCL–RuPt	71.2 ± 3.1

Solid-state UV–vis measurements using an integrating sphere revealed markedly different photostabilities for the two polymer matrices. PAN–RuPt membranes exhibited only minor RuPt loss upon red-light irradiation (11.7 ± 9.5%), whereas PCL–RuPt membranes showed pronounced loss (71.2 ± 3.1%).

4.10 Determination of LogP (Octanol/Water Partition Coefficient)

The octanol/water partition coefficient (logP) of RuPt was determined using a shake-flask method. A concentrated stock solution of RuPt in DMF was introduced into water (1 mL), followed by the addition of n-octanol (1 mL). The biphasic system was vigorously mixed to ensure thorough distribution of the compound between the two phases and subsequently kept in the dark for 24 h to allow complete phase separation.

After equilibration, aliquots (100 µL) from each phase were withdrawn separately and diluted with DMF (1200 µL). The absorbance spectra of the diluted samples were recorded by UV–vis spectroscopy.

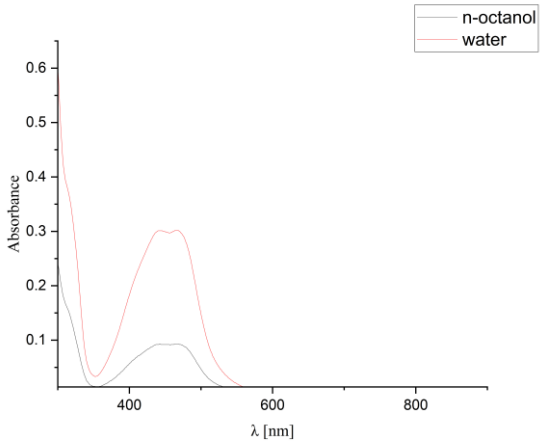

Fig. S35. Absorbance spectra of the n-octanol and H_2O phase for RuPt. Here, RuPt is more soluble in water than in octanol.

4.11 Energy-Dispersive X-ray Spectroscopy (EDS) Spectra and Composition Table

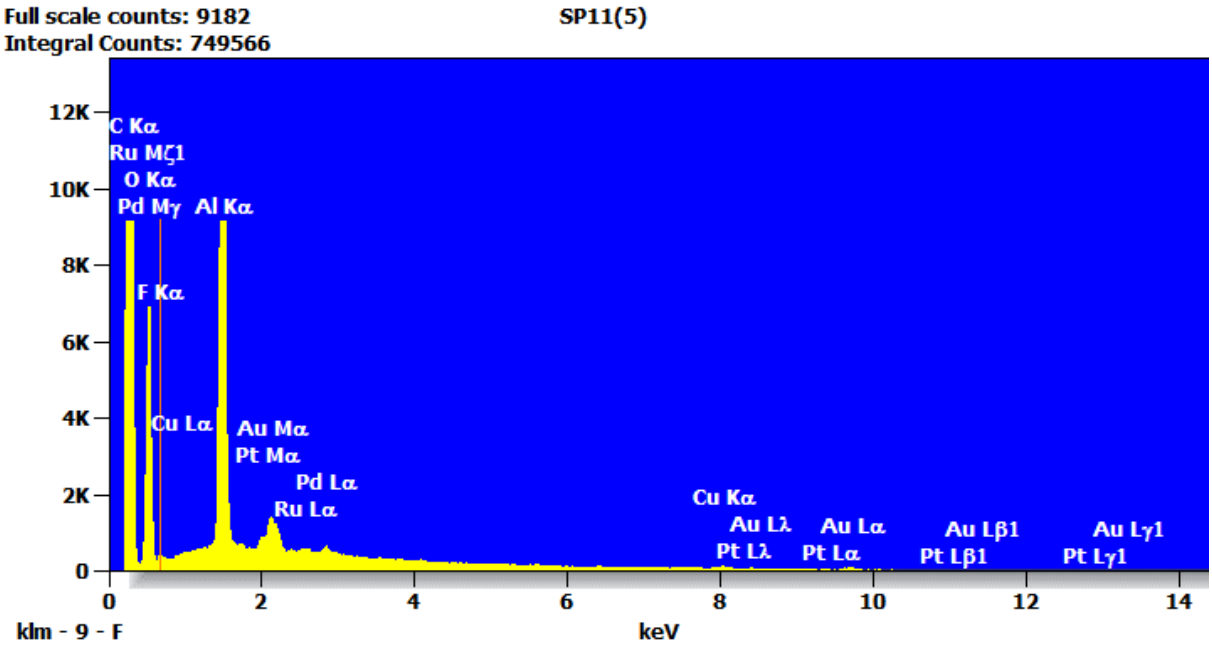

Element	Net Counts	Weight %	Weight % Error	Atom %	Atom % Error
C	297022	69.6	± 0.3	75.9	± 0.4
O	40887	28.8	± 0.2	23.6	± 0.2
F	1127	0.6	± 0.1	0.4	± 0.1
Ru	1763	0.3	± 0.1	0.0	± 0.0
Pt	3353	0.6	± 0.1	0.0	± 0.0
Total		100.0		100.0	

Fig. S36. EDX spectra and Quantitative Results for PAN-RuPt.

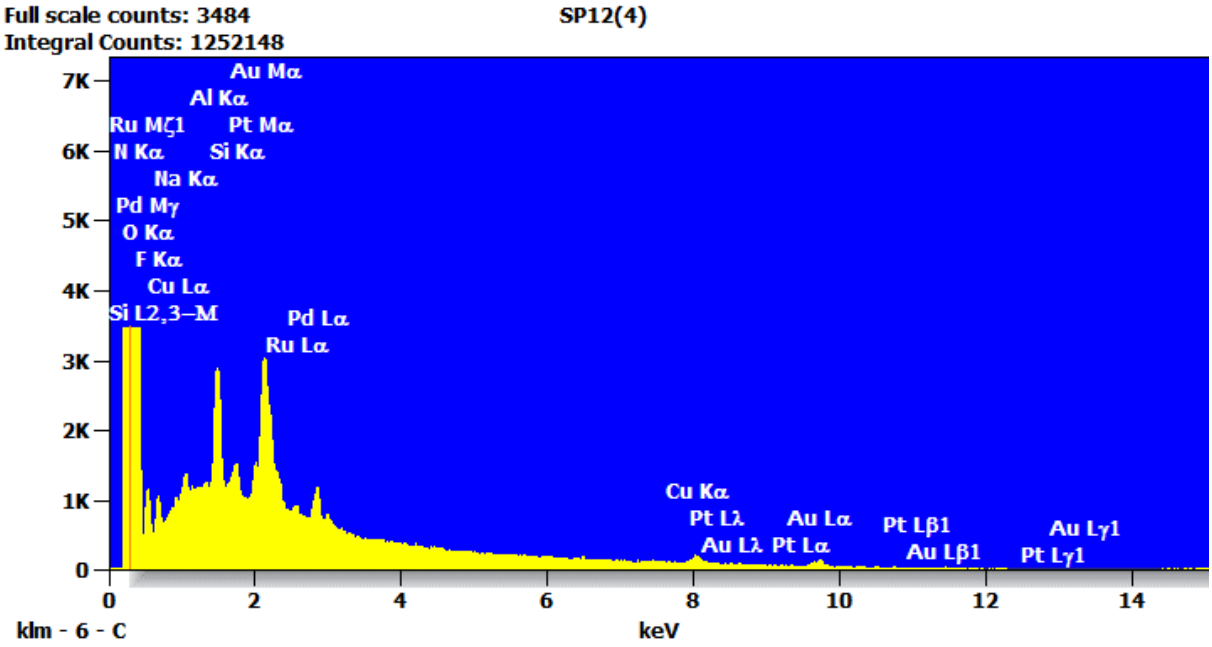

Element	Net Counts	Weight %	Weight % Error	Atom %	Atom % Error
N	19202	40.6	± 0.9	49.8	± 1.1
O	10309	30.4	± 0.8	32.7	± 0.9
F	6306	15.4	± 0.4	13.9	± 0.4
Na	2100	1.6	± 0.1	1.2	± 0.1
Si	4379	1.9	± 0.1	1.2	± 0.1
Ru	4517	3.9	± 0.3	0.7	± 0.1
Pt	7096	6.1	± 0.3	0.5	± 0.0
Total		100.0		100.0	

Fig. S37. EDX spectra and Quantitative Results for PCL-RuPt.

5. Biocompatibility

5.1 Cell Culture

Human fibroblast (GM-5657) cells were cultured in DMEM medium (1 g/L d-glucose) supplemented with 10% FBS superior, 2.4% penicillin/streptomycin, 1.2% GlutaMAX, and 1% sodium pyruvate. LGC Standards Ltd. provided the cell line, which was cultured at 37 °C with 10% CO_2. Before each experiment, the cells were passaged at least 3 times.

5.2 Cytotoxicity on Cell Monolayers

A total of 35×10^3 cells were seeded onto 24-well plates and allowed to adhere overnight. RuPt-PCL and RuPt-PAN membranes were disinfected in 70% ethanol for 3 h and thoroughly rinsed with PBS. The cells were then treated with the membranes, with a final volume of 1 mL per well, for 1 h at 37 °C and 5% CO_2. After this time, the membranes were removed, and the cells were incubated for an additional 44 h at 37 °C and 5% CO_2. After the specified incubation period, the culture medium was substituted with phosphate-buffered saline containing 3-(4,5-dimethylthiazol-2-yl)-2,5-diphenyltetrazolium bromide (MTT) with a final concentration of 12 µM. The cells were incubated for 2 h at 37 °C and 5% CO_2, and the mixture was replaced with 200 µL of DMSO. The concentration of the formazan dissolved in DMSO was determined with an Infinite M Nano plus Microplate reader (Tecan).

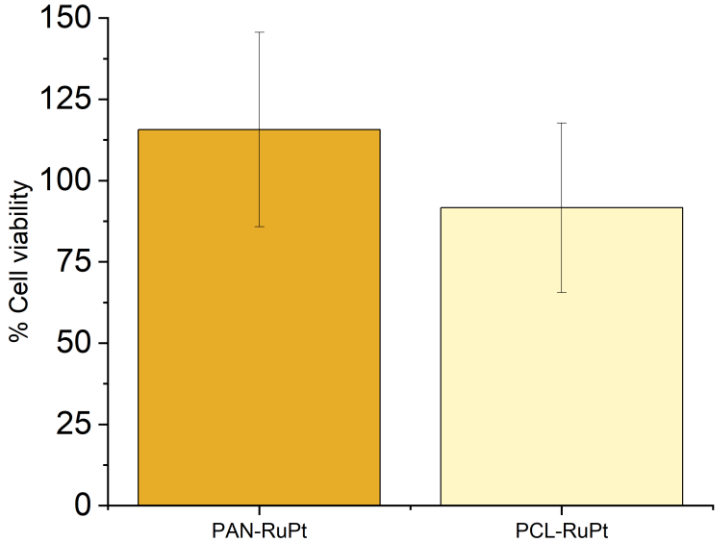

Fig. S38. Cell viability of GM-5657 cells after treatment with PAN-RuPt and PCL-RuPt membranes for 1 hour. Viability was determined by MTT assay and normalized to untreated control cells. Data are shown as mean ± SD from 8 technical replicates distributed across three plates.

6. Photobiological studies

6.1 General

B. subtilis strain DM10 and *E. coli* strain Nissle 1917 were grown on lysogeny broth (LB) agar and kept at 4°C. A single isolated colony was picked from this plate, transferred to 3 ml LB broth, and incubated aerobically overnight at 37°C in a shaker incubator at 180 rpm (rotations per minute). The following day, bacteria were suspended in 10 mL of fresh LB medium to an optical density OD_{600} = 0.1 and grown in a flask to attenuate of approximately OD_{600} = 0.4. Thereafter, the bacterial suspensions were centrifuged at 4000 rpm for 5 min, resuspended in a buffer solution to the final bacterial concentration of approximately $1x10^{-7}$ cells per mL, and used for the experiments.

6.2 Photoinactivation of bacteria and durability tests

To obtain a constant area of approximately 113 cm^2, samples were randomly cut from the electrospun mat at different locations using a 12 cm diameter hole punch. Before irradiation experiments, nanomaterials were treated with 70% aqueous ethanol solution overnight and then washed with a sufficient amount of PBS to disinfect them and remove unbound PSs. Each 12 mm diameter punch was incubated with 300 µL bacterial suspension for 15 min with and without 10 mM NaN_3 and irradiated with a LED array ranging from 465-660 nm light for a 1h. A power meter (Solar Meter from Solartech) was used to measure fluence rates regularly. After irradiation, viable bacterial cells were determined by serial dilutions of the bacterial suspension plated on Luria-Bertani agar plates. The plates were incubated at 37°C for 18h and the number of CFU/ml was calculated. For durability studies, irradiation experiment was repeated as described above using the membrane incubated with bacteria for 3 day and disinfected with 70% aqueous ethanol solution overnight before each experiment. Addition of NaN_3 alone with and without irradiation does not cause any significant change in bacterial viability.

6.3 Fluorescence and fluorescence lifetime imaging imaging

Fluorescence microscopy images were recorded using *Nikon inverted microscope TS2R* (*Nikon Corporation*, Tokyo, Japan) equipped with a IS-DMK33UX174 monochrom camera and a LED filter block. Bacterial suspensions labelled with live/dead staining kit (Invitrogen) in the dark for 15 min at rt. An aliquot of the sample was then transferred to an object slide and fluorescence images were recorded.

7. References

1 J. Sanz-Villafruela, L.-M. Servos, N. Montesdeoca, J. V. Cuevas-Vicario, A. J. Moro, J. C. Lima, M. Martínez-Alonso, G. Espino and J. Karges, *Inorg. Chem. Front.*, 2025, **12**, 5770–5782.

2 B. P. Sullivan, D. J. Salmon and T. J. Meyer, *Inorg. Chem.*, 1978, **17**, 3334–3341.